Loudspeaker Nonlinearities – Causes, Parameters, Symptoms

Wolfgang Klippel, Klippel GmbH, Dresden, Germany, klippel@klippel.de

ABSTRACT

The paper addresses the relationship between nonlinear distortion measurement and nonlinearities which are the physical causes for signal distortion in loudspeakers, headphones, micro-speakers and other transducers. Using simulation techniques characteristic symptoms are found for each nonlinearity and presented systematically in a guide for loudspeaker diagnostics. This information is important for the interpretation of nonlinear parameters and for performing measurements which describe the loudspeaker more comprehensively. The practical application of the new techniques are demonstrated on three different loudspeakers.

1. INTRODUCTION

Loudspeakers and other kinds of actuators which produce sound or vibrations behave differently at small and high amplitudes. The dependency on the amplitude is an indication for nonlinearities inherent in the system. A second nonlinear effect is the generation of additional spectral components which are not in the exciting stimulus. Those components may be interpreted as harmonic and intermodulation distortion and are the basis for traditional measurement techniques. The results of nonlinear distortion measurements highly depends on the properties of the stimulus such as the selected frequency, amplitude and phase of the exciting tones. The results can not describe the large signal performance completely but have to be understood as symptoms. This is the major difference to the small signal domain where a linear transfer function or impulse response describes the input/output relationship completely.
Measurements which rely on symptoms are problematic in the following way:
Does the measurement technique activate and detect significant symptoms of the loudspeaker ?
Are the symptoms meaningful and how are they related with the physical causes ?
How can we keep the measurement time and effort low while ensuring a comprehensive set of data ?

These questions will be addressed in the following paper. Answers will be derived from loudspeaker modeling and practical measurements. At the beginning the basic nonlinear mechanisms in loudspeakers are discussed. In a second part traditional and new measurement techniques are summarized. After discussing general symptoms related with the nonlinear curve shape the particular symptoms of dominant nonlinearities in loudspeakers are discussed systematically. It is the goal of the paper to provide a simple guide for assessing the large signal performance of loudspeakers. In the remaining part of the paper this guide will be applied to diagnose 3 loudspeakers intended for home and automotive applications. Finally, conclusion are drawn for practical work and further research.

2. GLOSSARY OF SYMBOLS

AMD	amplitude modulation distortion in percent
Bl(x)	is the effective instantaneous electro-dynamic coupling factor (force factor of the motor) defined by the integral of the permanent magnetic flux density B over voice coil length l.
C	amplitude compression of the fundamental in dB
E	envelope of a time signal
ETHD	equivalent total harmonic distortion at the transducer's terminals in percent
EHD_n	equivalent nth-order harmonic distortion at the transducer's terminals in percent
f_s	resonance frequency
FT	Fourier transform
$F_m(x,I)$	electro-magnetic driving force (reluctance force) due to the variation of the inductance versus x,
HD_n	nth-order harmonic distortion in percent
$H(j\omega)$	linear transfer function
ICHD	instantaneous crest factor of harmonic distortion in dB
IHD	instantaneous value of harmonic distortion component in percent
IMD_n	nth-order intermodulation distortion in percent
IMD_{total}	total harmonic intermodulation distortion in percent
i(t)	the electric input current,

$K_{ms}(x)$	mechanical stiffness of driver suspension which is the inverse of the compliance $C_{ms}(x)$,
$L_e(x,i)$ $L_2(x,i)$ $R_2(x,i)$	lumped parameters depending on displacement x and current i required to model the para-inductance of the voice coil ,
L_{AMD}	amplitude modulation distortion in decibel
$L_{HD,n}$	nth-order harmonic distortion in the sound pressure output signal in decibel
L_{THD}	total harmonic distortion in the sound pressure output in decibel
$L_{EHD,n}$	equivalent nth-order harmonic distortion in decibel
L_{ETHD}	equivalent total harmonic distortion in decibel
L_{THD}	equivalent total harmonic distortion in decibel
$L_{IMD,n}$	nth-order intermodulation distortion in the sound pressure output signal in decibel
$L_{IMD,total}$	total harmonic intermodulation distortion in the sound pressure output signal in decibel

M_{ms}	mechanical mass of driver diaphragm assembly including voice-coil and air load,
$p(t)$	sound pressure output
$P(j\omega)$	spectrum of sound pressure signal
P_n	nth-order harmonic component in sound pressure
P_t	rms-value of the total sound pressure signal
$P_r(f_1,U_i)$	relative amplitude of the fundamental (referred to a voltage U_i)
n	order of the distortion component
R_{ms}	mechanical resistance of driver suspension losses,
$R_e(T_V)$	DC resistance of voice coil,
THD	total harmonic distortion in the sound pressure output in percent
$u(t)$	the driving voltage at loudspeaker terminals.
$u_D(t)$	equivalent input distortion considering all nonlinearities
$u'(t)$	total equivalent input voltage $u'=u+u_D$
$v(t)$	velocity of the voice coil,
$x(t)$	displacement of the voice coil,
$Z_m(s)$	mechanical impedance representing mechanical or acoustical load.

3. LOUDSPEAKER MODELING

The traditional linear model fails in explaining the behavior of loudspeakers at high amplitude. The development of nonlinear loudspeaker models is complicated and most of the research is focused on the “dominant nonlinearities” which

- limit acoustical output
- generate audible distortion
- indicate an overload situation
- cause unstable behavior
- are related with cost, weight, volume

- determine transducer efficiency
- affect loudspeaker system alignment.

The dominant nonlinearities found in woofer, tweeter, micro-speaker, horn compression driver and loudspeaker system are summarized in Table 1 and discussed in the following chapter in greater detail.

NONLINEARITY	**EFFECT**	**MULTIPLIED TIME SIGNALS**
Stiffness $K_{ms}(x)$ of the suspension	nonlinear restoring force $F_s=K_{ms}(x)x$	displacement x
Force factor $Bl(x)$	driving force $F=Bl(x)i$ causes parametric excitation	displacement x current i
	back EMF $u_{EMF}=Bl(x)v$ causes nonlinear damping	displacement x velocity v
Inductance $L_e(x)$ (magnetic ac-field varies with coil position)	time derivative of magnetic flux $\Phi_x=L(x)i$ produces back-induced voltage	displacement x current i
	additional reluctance force $F_m \sim i^2$ driving the mechanical system	current i
Inductance $L_e(i)$ (magnetic ac-field changes permeability of the magnetic circuit)	time derivative of magnetic flux $\Phi_i=L(i)i$ produces back-induced voltage	current i
Young's modulus $E(\varepsilon)$ of the material (cone, surround)	stress in the material $\sigma=E(\varepsilon)\varepsilon$ is a nonlinear function of strain	strain ε
geometrical transfer matrix	geometry is changed by mechanical vibration	strain vector ε
Flow resistance $R_p(v)$ of the port in vented cabinets	sound pressur inside the box is *a* nonlinear function of the air flow	air velocity v in the port
Doppler Effect (variation of the cone position)	variable time shift $\tau=x/c$ in the propagated signal causes phase distortion	displacement x sound pressure p
Nonlinear sound propagation	speed of sound $c(p)$ depends on pressure and	sound pressure p

	causes wave steepening	

Table 1 Overview on dominant nonlinearities in an electro-dynamical loudspeaker

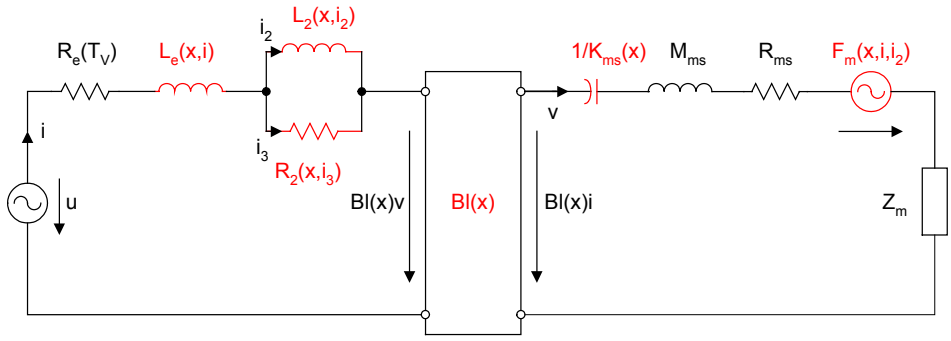

Figure 1: Electrical equivalent circuit of the electro-dynamical transducer

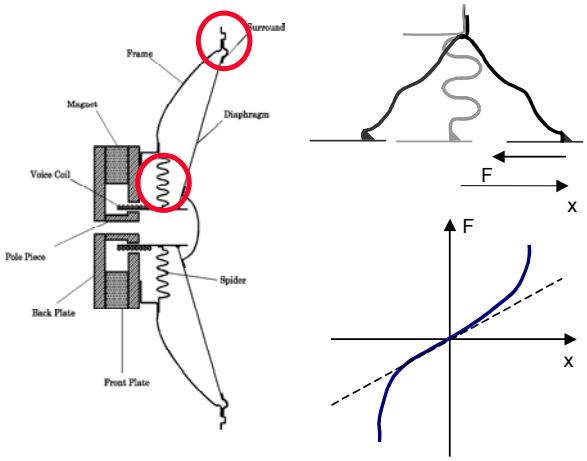

Figure 2: Suspension system in a conventional loudspeaker (sectional view) and the nonlinear force-deflection curve.

3.1.1. Nonlinear stiffness

Loudspeakers use a suspension system to center the coil in gap and to generate a restoring force which moves the coil back to the rest position. Woofers usually have a suspension comprising a spider and a surround as shown in Figure 2 which allows movements in one direction only and suppresses rocking modes.

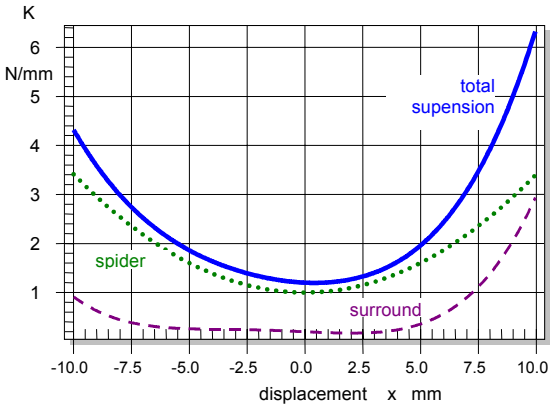

Figure 3: Stiffness of a progressive spider (dotted curve), a limiting surround (dashed curve) and the total suspension (solid curve)

Most of the suspension are made of impregnated fabric, rubber and plastic molded with a particular shape. Suspension behaves like a normal spring and may be characterized by the force-deflection curve as shown in Figure 2. There is an almost linear relationship at low displacement but at high forces the suspension gives less displacement than predicted by a constant spring constant. Applying an ac-force the displacement follows with a hysteresis which is caused by losses in the material.

The restoring force $F=K_{ms}(x)x$ may also be described by the product of displacement and nonlinear stiffness $K_{ms}(x)$. The stiffness $K_{ms}(x)$ corresponds with the secant between any point of the force-reflection curve and the origin. Since the stiffness is not constant but itself a function of the displacement x the restoring force contains products of voice coil displacement. These terms produce nonlinear distortion in the time signal which are typical for the suspension.

Figure 3 shows the $K_{ms}(x)$-characteristic of a spider with a progressive characteristic and a surround which limits the excursion at positive displacement.

3.1.2. Force Factor

The force factor *Bl(x)* describes the coupling between mechanical and electrical side of an electro-dynamical transducer. This parameter is the integral of the flux density *B* versus voice coil length *l*. The force *factor Bl(x)* is not a constant but depends on the displacement *x* of the voice coil. Clearly if windings of the coil leave the gap the force factor decreases. The nonlinear function is static (no frequency dependency) and can be represented as a nonlinear graph, table or power series expansion.

The shape of the *Bl(x)*-curve depends on the geometry of the coil-gap configuration and the *B*-field generated by the magnet. Figure 4 illustrates an overhang configuration where the coil height h_{coil} is larger than depth h_{gap} of the gap. The corresponding *Bl(x)*-curve is shown as solid line in Figure 5. For small displacement the force factor value is almost constant because the same number of windings is in the gap. A coil height equal with the coil depth corresponds with the dashed curve in Figure 5 where the force factor decreases without plateau already at low amplitudes.

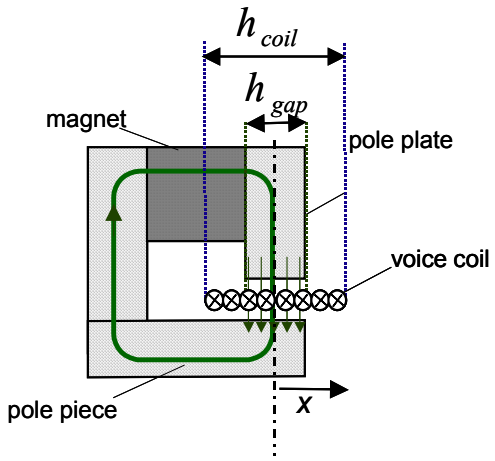

Figure 4: Motor structure of a of an overhang configuration

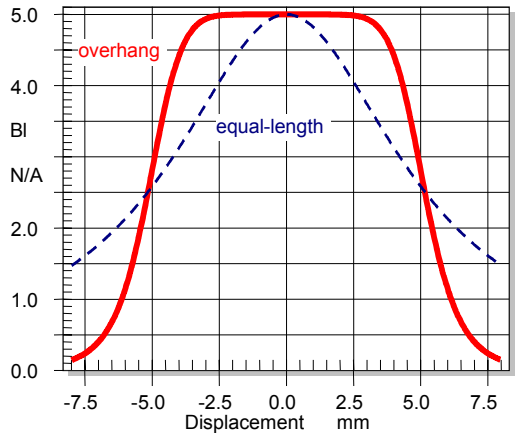

Figure 5: Force factor *Bl(x)* of an overhang and equal-length coil-gap configuration

The force factor *Bl(x)* has two nonlinear effects as listed in Table 1:

- As a coupling factor between electrical and mechanical domain any variation of *Bl(x)* will affect the electro-dynamical driving force *F=Bl(x)i.* This mechanisms is also called parametric excitation of a resonating system. High values of displacement *x* and current *i* are required to produce significant distortion.
- The second effect of the *Bl(x)* is the back *EMF* generated by the movement of the coil in permanent field. Here force factor *Bl(x)* is multiplied with the velocity and causes variation of the electrical damping.

3.1.3. Voice coil inductance

The electrical input impedance depends on the position of the coil. For example, Figure 6 shows the electrical input impedance versus frequency measured at three voice coil positions (x=0, clamped at +7 mm and –7 mm). Above the resonance at 70 Hz (which does not appear for a clamped voice coil) the electrical impedance is significantly higher for a negative displacement (coil in position) than at positive displacement (coil out position).

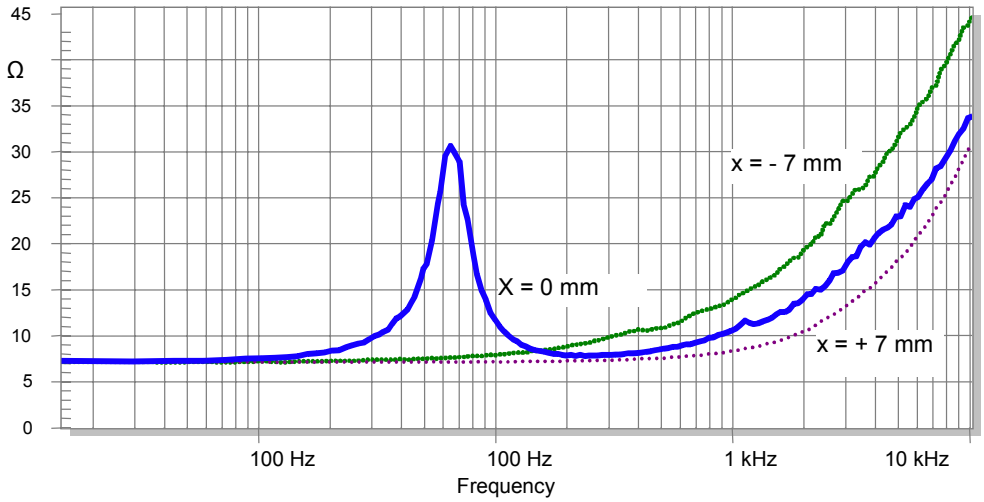

Figure 6: Electrical impedance measured at the rest position *(x=0)* and with clamped voice coil at positive and negative displacement.

This property can be observed on many loudspeakers and can be explained by the displacement varying inductance. The current in the voice coil also produces a magnetic ac-field penetrating the magnet, iron and air as shown in Figure 7. The magnetic flux depends on the position of the coil and the magnitude of the current. If the coil is in free air the inductance is much lower than operating the coil below the gap where the surrounding iron path decreases the magnetic resistance.

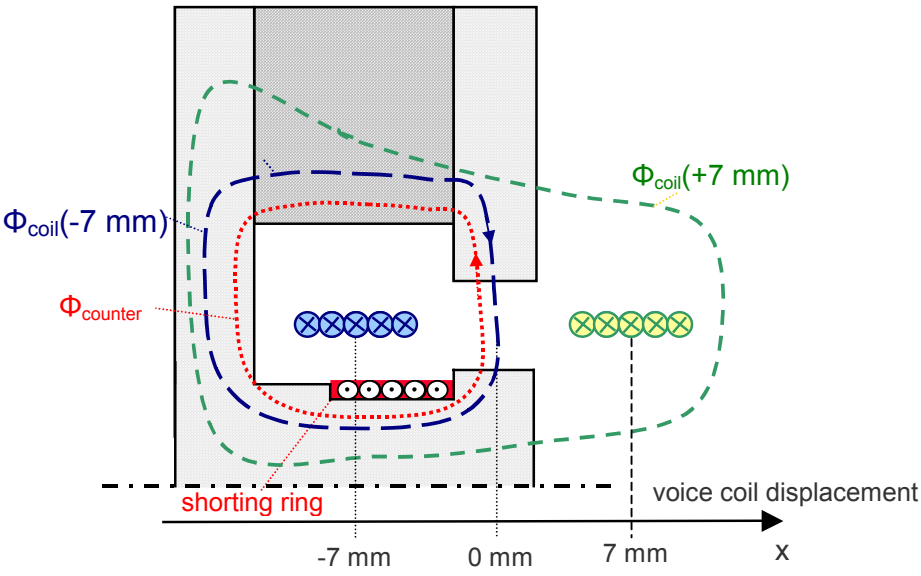

Figure 7: Motor structure of a conventional driver using a shorting ring on the pole piece.

In addition to the dependency of the inductance on displacement *x* there is also a dependency on the input current *i.* This is caused by the nonlinear relationship between magnetic field strength *H* and flux density (induction) *B* as shown in Figure 8. For no current the permanent magnet produces the field strength H_2 which determines the working point in the *B(H)*-characteristic. A high positive current (*i* = 10 A) increases the total field strength H_3 where the iron is more saturated and the permeability μ is decreased. Contrary at negative current *(i* = -10 A) the total field strength is decreased giving a higher value of μ. The effect of the varying permeability $\mu(i)$ is also called "flux modulation". The ac current also generates a hysteresis loop which corresponds with the losses in the iron material during one period of a sinusoidal current.

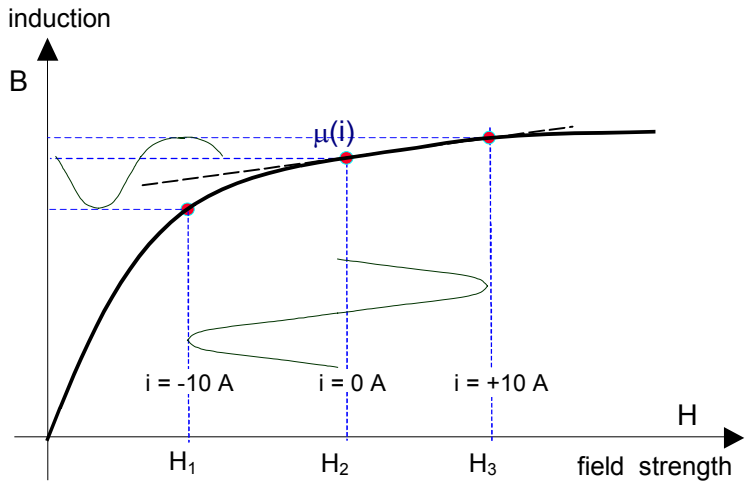

Figure 8: Flux density *B* versus magnetic field strength *H* of the magnetic circuit showing that the permeability $\mu(i)$ depends on the voice coil current *i*.

The magnetic ac-flux increases the impedance at higher frequencies as shown in Figure 6. This increase can not be described by an ideal inductance. Special models (Leach, Wright, cascaded LR-network) are required to describe losses generated by eddy currents in the iron material. The discrete model using an inductance $L_e(x,i)$ in series with a second inductance $L_2(x,i)$ shunted by a resistor $R_2(x,i)$ as shown in Figure 1 is a good candidate to consider the nonlinear dependency on displacement and current. The particular parameters depend on the frequency range over which the fitting is performed [1]. For most applications it is also convenient to use a simple approximation which neglect the nonlinear interactions between current and displacement and use the same nonlinear curve shape for the displacement varying parameters

$$\frac{L_e(x, i=0)}{L_e(0)} \approx \frac{L_2(x, i=0)}{L_2(0)} \approx \frac{R_2(x, i=0)}{R_2(0)}$$

and the current varying parameters

$$\frac{L_e(i, x=0)}{L_e(0)} \approx \frac{L_2(i, x=0)}{L_2(0)} \approx \frac{R_2(i, x=0)}{R_2(0)}.$$

This approximation reduces the amount of data used in loudspeaker diagnostic and loudspeaker design. The nonlinear characteristics of $L_e(x)$ versus displacement *x* and $L_e(i)$ versus i and the values $L_2(0)$ and $R_2(0)$ at the rest position $x=0$ are sufficient in most applications to describe the nonlinear characteristic of the para-inductance. For example, the Figure 9 and Figure 10 show the dependency of the $L_e(x)$ and $L_e(i)$ versus displacement and current, respectively.

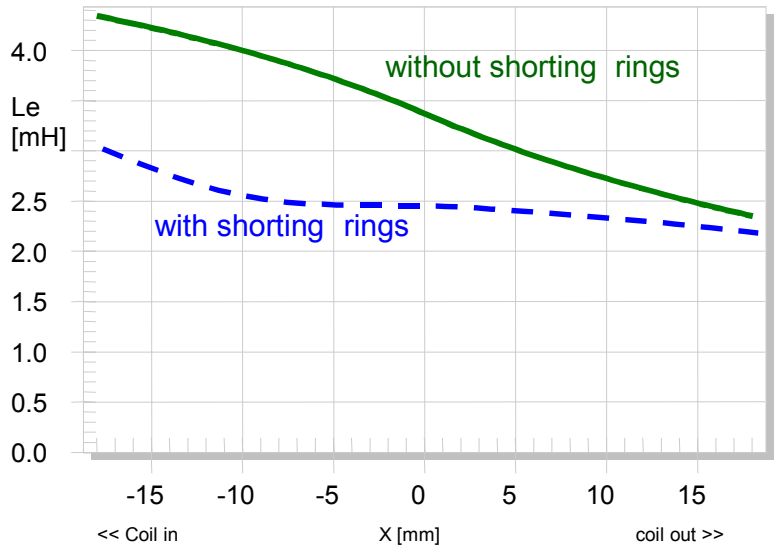

Figure 9: Voice coil inductance $L_e(x, i=0)$ versus displacement x for a motor with and without shorting rings

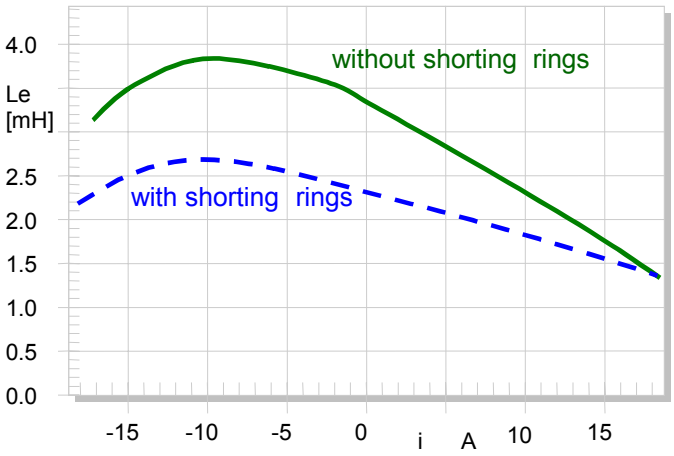

Figure 10: Voice coil inductance $L_e(i, x=0)$ versus voice coil current i with and without shorting rings

The inductance of the coil can be significantly reduced by placing conductive material (usually rings or caps made of aluminum or copper) on the pole piece or close to the coil as shown in Figure 7. The ac-field induces a current in the shorting material which generates a counter flux and reduces the total flux and the inductance of the coil. This arrangement behaves very similar to a transformer which is shorted at the secondary side.

If the shorting material is placed at points where the inductance is maximal, the $L_e(x)$-curve can significantly linearized as shown as dashed line in Figure 9. Using shorting material has also a positive effect on the $L_e(i)$-characteristic because the ac-field field is smaller and produces less flux modulation.

Table 1 summarizes the nonlinear effects and shows which time signals are multiplied with each other:

- The first effect of the displacement varying inductance $L_e(x)$ is the back induced voltage in the electrical input circuit due to the time derivative of the magnetic flux and leads to the variation of the input impedance as shown in Figure 6. This effect causes a multiplication of displacement and current. The same signals are involved in the parametric excitation of the $Bl(x)$ but there is an additional differentiation after the multiplication which enhances the amplitude of the components by 6dB/octave to higher frequencies.

- The second effect is an additional reluctance force $F_m(x,i,i_2)$ which drives the mechanical system directly as shown in the equivalent circuit in Figure 1. It can be approximated by

$$F_m(x,i,i_2) \approx -\frac{i(t)^2}{2}\frac{\partial L_e(x)}{\partial x} - \frac{i_2(t)^2}{2}\frac{\partial L_2(x)}{\partial x}.$$

  The reluctance force multiplies the local derivative of $L_e(x)$ with the squared current. The squarer is the dominant nonlinear operation and generates distortion in the full audio band. The reluctance force is the major driving force in electro-magnetic loudspeaker used 50 years ago. In current electro-dynamical transducers the reluctance force is an undesired rudiment which should be as low as possible.

- The dependency of $L_e(i)$ versus current cause an ac-flux which depends on powers of i. Since the current is a broad band signal, distortion components are generated in the full audio band.

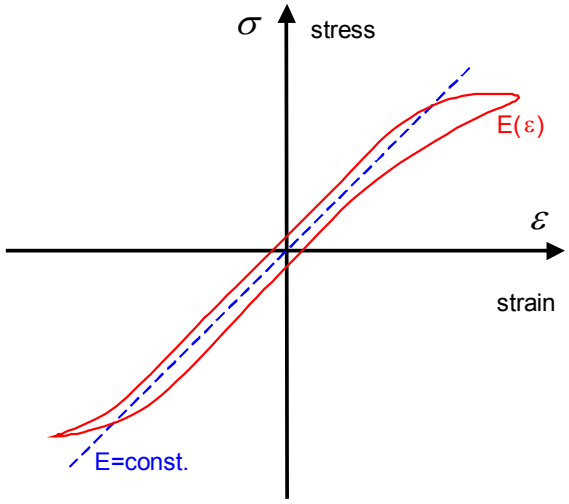

Figure 11: Nonlinear material properties as causes for nonlinearities in the mechanical system

3.1.4. Nonlinear Material properties

At low frequencies where the cone vibrates as a piston the suspension is the only nonlinear part of the mechanical system and can be described by a single lumped parameter $K_{ms}(x)$. At higher frequencies break-up modes occur on cone and other parts (voice coil former, dust cap). These vibrations become nonlinear if the strain and stress in the material is very high and Young's modulus $E(\varepsilon)$ varies with the strain ε.

Nonlinear distortion are generated in the stress σ due to the multiplication of $E(\varepsilon)$ with the strain ε becomes maximal at distinct frequencies (Eigenfrequencies) where the modes produce high strain in the material [2].

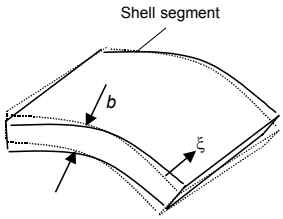

Figure 12: Variation of the cone geometry due to mechanical vibration

3.1.5. Variation of Geometry

More important than the variation of the *E*-modul is the variation of the geometry of the mechanical system. The vibration becomes nonlinear if the displacement ζ is not small in comparison to geometrical dimensions (e.g. thickness b or curvature of the cone segment [3]) as illustrated in Figure 12.

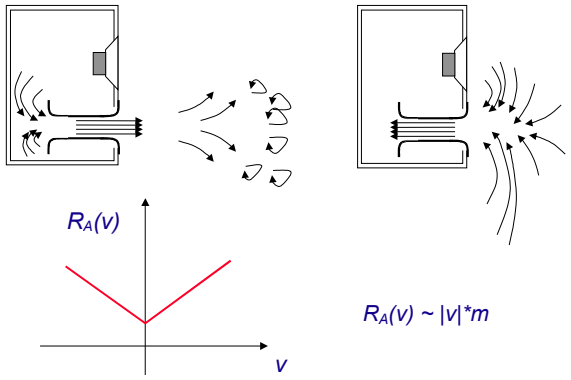

Figure 13: Nonlinear flow resistance depends on the air velocity

3.1.6. Port nonlinearity

Ports in vented system have a flow resistance which is not constant but highly depends on the velocity *v* of the air inside the port [4] . At very low amplitudes the loss factor of a normal port is very high ($Q > 50$) but this values goes down to 10 and less for particle velocities above 20 m/s. The reason is that the air in the port does not vibrate as an air plug where all the air particles are bounded together. During the out-breathing phase the air is pushed in axis into the far field. In the following in-breathing phase other air particles resting around the orifice are accelerated and sucked into port. The kinetic energy moved into the far field corresponds with the increase of the flow resistance for positive and negative air velocities as illustrated in Figure 13.

The nonlinear flow resistance $R_p(v)$ generates low frequency components because the velocity is multiplied with each other. An asymmetry in $R_p(v)$ caused by the geometry of the orifices generates a dc-pressure in the box which may spoil the voice coil position and cause motor distortion eventually.

A second nonlinear mechanism is the generation of turbulences in the air flow which causes broad band noise in the output signal [5].

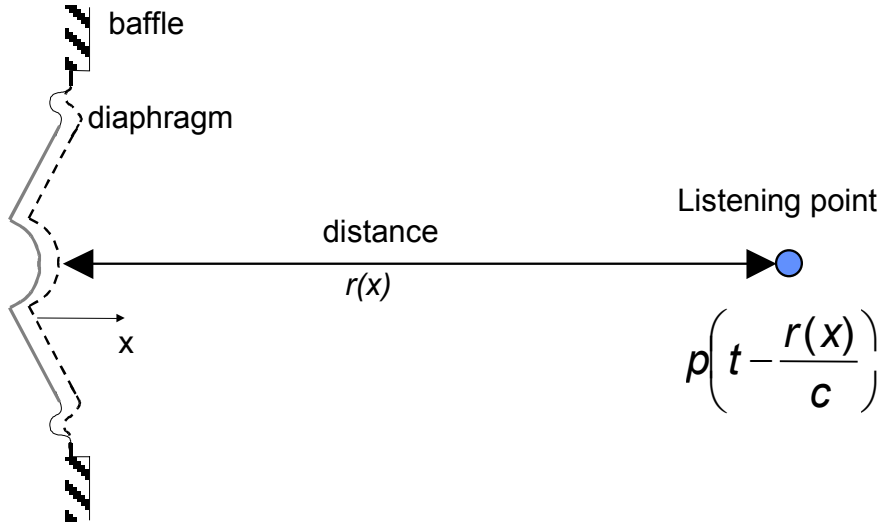

Figure 14: Phase modulation caused by varying distance between cone and listening point (Doppler Effect)

3.1.7. Doppler Effect

Variation of the position and geometry of the cone and surround does not only affect the mechanical vibration but also the acoustical radiation condition [10]. The Doppler Effect is the most dominant nonlinearity in this group. The voice coil displacement generated by a low frequency component varies the distance between the radiating surface (cone) and a listening point in axis. The varying time delay in the sound pressure signal can be interpreted as a phase or frequency modulation [9]. This is not very critical for the low frequency component itself but causes high intermodulation of high frequency signals with a short wavelength. This mechanism may be described by the product of displacement and differentiated sound pressure and requires low and high frequency components at the same time. The easiest way to avoid this distortion is to use a multi-way system with a sufficiently low crossover frequency between woofer and tweeter system.

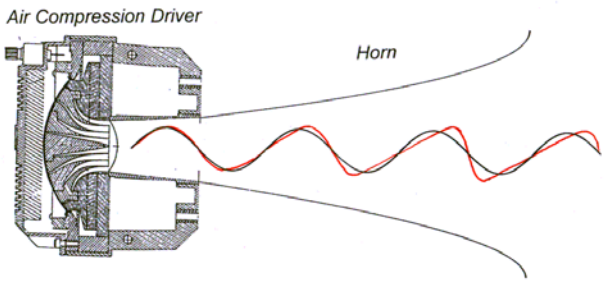

Figure 15: A sound wave propagating at high amplitudes causes a characteristic steepening of the wave front

3.1.8. Wave Steepening

At high amplitudes a sound wave propagates at the maxima faster than at the minima causing a gradual steepening of the wave front [6]. This mechanism is found in horn loaded compression drivers. The nonlinear mechanism is basically a multiplication of the sound pressure with the differentiated sound pressure in each section of the horn [7].

3.2. Measurement of model parameters

Modeling becomes practical if the free parameters of the model can be identified on a particular unit. The parameters of the lumped parameter model in Figure 1 can be measured by using static, incremental dynamic [11] or full dynamic techniques [12]. The static and the incremental dynamic methods use a dc-part in the stimulus to operate the loudspeaker in a particular working point. However, only a full dynamic measurement technique operates the loudspeaker under normal working conditions and can use an audio-signal as stimulus. This is important for considering visco-elastic effects of the suspension [16] and for measuring the inductance $L_e(i)$ up to a high currents (> 30 Ampere) where heating of the coil may damage the loudspeaker. In this paper all large signal parameters are measured dynamically by using the system identification technique (LSI of the Distortion Analyzer [20]).

3.3. Simulation of signal performance

If the loudspeaker model is adequate and the free parameters are measured carefully the behavior of the loudspeaker may be predicted for any input signal (synthetic test signal or music as stimulus). The simulation does not need a sensor but gives access to all state variables of the system (sound pressure, current, displacement,..). It is also possible to separate nonlinear distortion of each nonlinearity from the linear output and to measure the magnitude of the distortion in an audio signal at any time. Modeling is

also the basis for a new auralization technique [22] which combines objective and subjective assessment of the large signal performance.

4. MEASUREMENT OF SYMPTOMS

The traditional way of assessing the large signal performance is the measurement of special symptoms generated by the nonlinear system at high amplitudes. Such symptoms are:

- generation of new spectral components in the output signal (which can be identified as harmonic, sub-harmonic and intermodulation components)
- Nonlinear relationship between the amplitude of the input and output amplitude of fundamental and distortion components ("nonlinear amplitude compression")
- Generation of a dc-part in the state variables (e.g. dc-displacement)
- Instabilities leading to bifurcation and jumping effects.

Those symptoms give valuable information about:

- deviation from linear behavior (almost linear, weak nonlinear or strong nonlinear behavior)
- physical nature of the nonlinearity (e.g. force factor)
- shape of the nonlinear characteristic
- quantitative identification of nonlinear parameters.

4.1. Critical stimulus

Symptoms are only generated if the nonlinearities are activated by an appropriate stimulus. Since the nonlinearities of the motor and suspension are relatively smooth curves, the loudspeaker behaves almost linear for sufficiently small amplitudes. High displacement is required to cause significant variation of the force factor $Bl(x)$, inductance $L_e(x)$ and stiffness $K_{ms}(x)$. Therefore the stimulus should provide sufficient energy at frequencies below $2f_s$ because the displacement decreases by 12 dB/octave above resonance frequency f_s. The current varying inductance $L_e(i)$ requires high voice coil current. Due to the electrical input impedance the current is high at low frequencies, becomes minimal at the resonance, increases to high values again at $2f_s$ and gradually decays at higher frequencies.

Variation of the nonlinear parameters is not a sufficient condition for the generation of the nonlinear distortion. Furthermore the second signal which is multiplied with the

nonlinear parameter should have high amplitude. That means that the nonlinear terms in Table 1 which multiply two different time signals require a stimulus which produces high amplitudes of both state variables at the same time. In some cases this can not be accomplished by a single tone. For example the L(x)-nonlinearity requires at least a low frequency tone for generating displacement and a high frequency tone for generating sufficient current. A two-tone stimulus has the advantage over a multi-tone signal that the generated components can be separated in the frequency domain to simplify the identification and interpretation.

4.2. Monitoring of State Variables

The sound pressure output measured by a microphone is of course the most natural candidate for monitoring the state of the loudspeaker. However, cone vibration radiation, the room and ambient noise have an influence on the signal. Monitoring the voice coil displacement by a triangulation laser sensor is a more direct way of observing the state of the suspension and motor. In the displacement a considerable dc-component may be generated by asymmetrical nonlinearities (rectification process). The input current is also a very informative state signal and can also easily be measured. The dynamic measurement of the large signal parameters in the LSI module [20] is based on monitoring electrical signals at the loudspeaker terminals only. Monitoring the voltage at the terminals is useful if the loudspeaker is operated via a high impedance amplifier (current source). Monitoring of velocity and cone acceleration can be accomplished by using an expensive Doppler laser system or an inexpensive accelerometer mounted on the cone.

4.3. Signal Analysis and Distortion Measures

A nonlinear system excited by a two-tone stimulus $u(t)= 1.4U_0 \sin(2\pi f_1 t)+1.4U_0 \sin(2\pi f_2 t)$ with a first excitation tone at frequency f_1 and a second tone at f_2 generates a state variable (e.g. sound pressure $p(t)$) which is applied to a spectral analysis (Fourier transform $\boldsymbol{FT}$) giving the spectrum (e.g $P(j\omega)=\boldsymbol{FT}\{p(t)\}$).

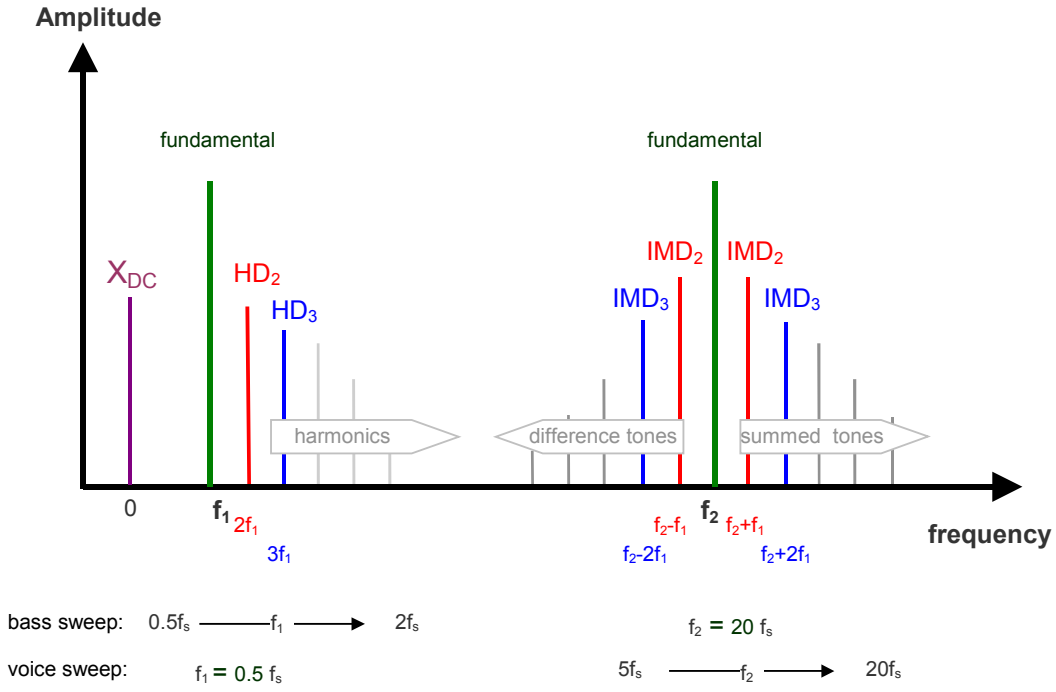

Figure 16 Spectrum of a state variable (e.g. sound pressure, displacement, current) generated by a two-tone stimulus

If the distance between the two tones is sufficiently high (f_2 >> f_1) the fundamental components, harmonic and intermodulation components are nicely separated and can be easily identified as illustrated in Figure 16.

4.3.1. Fundamental Components

The complex spectrum $P(j\omega)=FT\{p(t)\}$ comprises the fundamental components $P(j\omega_1)$ and $P(j\omega_2)$. While performing a series of measurement with varied frequency f_1 the amplitude and phase response of the fundamental component can be measured in the interested frequency range. In contrast to the linear transfer response measured at sufficiently small amplitudes the large signal response depends on the amplitude and the spectral content of the stimulus. Thus the second tone at f_2 may influence the amplitude of the output component at f_1. In the paper all measurements of the fundamental components are performed with a single tone f_1.

Although the phase response changes significantly at higher amplitude it plays a minor role in loudspeaker diagnostics so far.

More important is the relationship between input and output magnitude which reveals the nonlinear amplitude compression. In practice a series of measurements *i= 1, ... N* is performed while changing the amplitude of the input signal U_o=*i*ΔU* and calculating the relative amplitude

$$P_r(f_1,U_i)=\frac{|P(j2\pi f_1)|}{U_i}U_1\,. \tag{1}$$

The measure $P_r(f_1, U_i)$ is a convenient basis for comparing all measurements in one diagram and for calculating the amplitude compression

$$C(f_1,U_i)=20\lg\left(\frac{P_r(f_1,U_1)}{P_r(f_1,U_i)}\right). \tag{2}$$

4.3.2. Harmonic Distortion

The 2nd-order, 3rd-order and higher-order harmonic components $P_n(j\omega_1)=0.7P(nj\omega_1)$ with $n > 1$ appear at $2f_1$, $3f_1$ and multiples $nj\omega_1$ of the fundament frequency f_1. The harmonics of the second tone f_2 are at higher frequencies which are not shown in Figure 16. According to the IEC standard [13] the nth-order **H**armonic **D**istortion may be expressed in percent

$$HD_n=\frac{|P_n|}{P_t}100 \tag{3}$$

or in decibel

$$L_{HD,n}=20\lg\left(\frac{HD_n}{100}\right), \tag{4}$$

the **T**otal **H**armonic **D**istortion in percent

$$THD=\frac{\sqrt{\sum_{i=2}^{N}|P_i|^2}}{P_t}100 \tag{5}$$

or in decibel

$$L_{THD}=20\lg\left(\frac{THD}{100}\right) \tag{6}$$

using the rms-value of the total signal

$$P_t=\sqrt{\frac{1}{T}\int_0^T p(t)^2\,dt}\,. \tag{7}$$

The way how harmonic distortion are commonly presented has some disadvantages:

The measures $HD_{n,}$ THD in Eqs. (3) and (5), respectively, refer the amplitude of the measured distortion components to the rms-value P_t of the total signal $p(t)$. In this way the measured distortion responses depend on the fundamental which is mainly determined by the linear transfer function $H(j\omega)$. This causes high values of harmonic distortion at low frequencies where the radiation of the harmonics is much better than the radiation of the fundamental. Also break up modes, radiation, deflections of the sound wave at the enclosure and reflection in the room acoustics increase the complexity of the distortion curves.

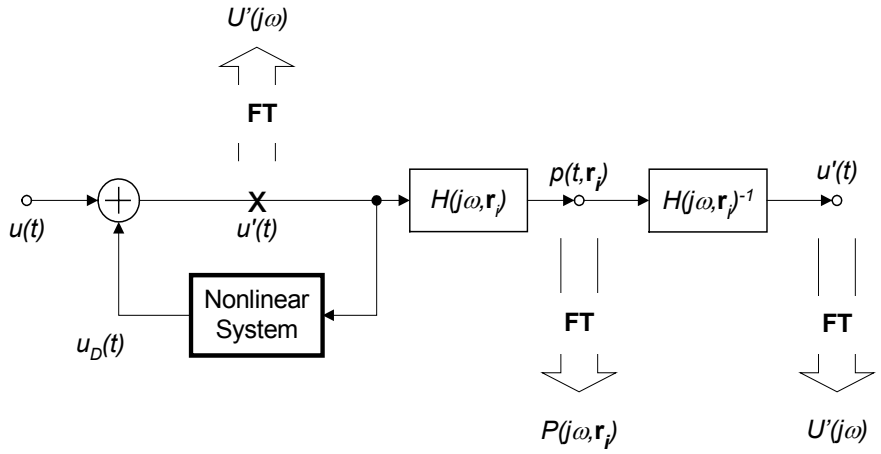

Figure 17: Measurement of equivalent input distortion by performing an inverse filtering prior to spectral analysis.

The results of the distortion measurement are much easier to interpret if the distortion are measured closer to the source. Since most of the dominant distortion is generated in the one-dimensional signal path (motor, suspension) it can be lumped together to a signal source adding distortion $u_D(t)$ to the input signal $u(t)$, as shown in Figure 17. Unfortunately, this point is not accessible for direct measurements in real loudspeakers. However, distortion measured in sound pressure, displacement or any other state variable can easily be transformed into the input signal by filtering with the inverse transfer function $H(j\omega)^{-1}$. This concept [14] produces less but more meaningful data and is a convenient way for separating motor distortion from distortion generated in the multi-dimensional domain (break-up modes, radiation).

The *nth*-order **E**quivalent **H**armonic **I**nput **D**istortion in percent is defined in percent

$$EHD_n = \frac{|U_n|}{U_t} 100 \ , \quad \text{for } n > 1 \tag{8}$$

or in decibel

$$L_{EHD,n} = 20\lg\left(\frac{EHD_n}{100}\right), \quad \text{for } n > 1, \tag{9}$$

the **E**quivalent **T**otal **H**armonic **I**nput **D**istortion in percent

$$ETHD = \frac{\sqrt{|U_2|^2 + |U_3|^2 + \ldots |U_3|^2}}{U_t} 100 \tag{10}$$

or in decibel

$$L_{ETHD} = 20\lg\left(\frac{ETHD}{100}\right) \tag{11}$$

using the equivalent input components

$$U_n(j\omega_1) = \frac{P_n(j\omega_1)}{H(nj\omega_1)}, \; n > 0 \tag{12}$$

and the rms value of the total voltage signal U_t

$$U_t = \sqrt{\frac{1}{T}\int_0^T u(t)^2 + u_D(t)^2\, dt}\,. \tag{13}$$

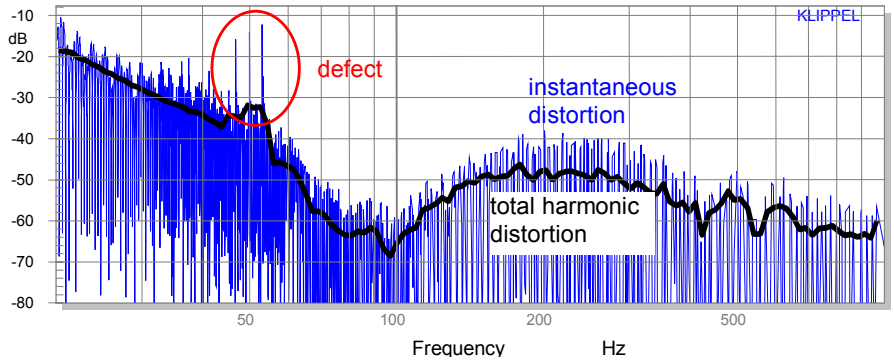

Figure 18: Instantaneous distortion IHD and total harmonic distortion THD in sound pressure output measured with a sinusoidal sweep.

Traditional harmonic distortion measurement only exploits the amplitude of the harmonic components. The phase of the higher-order harmonics is usually neglected because the interpretation is difficult. However, both phase and amplitude spectrum determine the waveform of the distortion in the time domain [21] . The waveform of the harmonic distortion signal can be calculated for a sinusoidal stimulus at ω by applying

the inverse Fourier transform to the harmonics in the complex spectrum giving the **I**nstantaneous **H**armonic **D**istortion in percent

$$IHD(t) = \frac{\left| \sum_{i=2}^{N} P_i e^{ji\omega t} + P_i^* e^{-ji\omega t} \right|}{p(t)} 100 \tag{14}$$

or in decibel

$$L_{IHD} = 20 \lg\left(\frac{IHD}{100} \right). \tag{15}$$

For a sinusoidal sweep the time *t* corresponds with an instantaneous frequency ω(t) giving the frequency response $L_{IHD(f)}$. For example, Figure 18 shows instantaneous harmonic distortion $L_{IHD(f)}$ as thin line and the total harmonic distortion *THD* as thick line versus frequency between 20 Hz and 1 kHz. The ratio between the instantaneous distortion (*IHD*) and the rms-value of the distortion (*THD*) gives the **I**nstantaneous **C**rest factor of **H**armonic **D**istortion

$$ICHD = 20 \lg\left(\frac{IHD}{THD} \right) . \tag{16}$$

in decibel. This measure describes the transient and impulsive properties of the harmonic distortion and plays an important role for the separation of soft- or hard limiting nonlinearities and the identification of loudspeaker defects. For example, distortion caused by regular motor and suspension nonlinearities produce relatively smooth distortion and the *ICHD* stays below 10 dB. A loudspeaker defect such as a wire beat generates a much higher crest factor (*ICHD* > 10 dB) as shown at 50 Hz in Figure 18.

4.3.3. Intermodulation Distortion

The IEC standard [13] summarizes the summed and difference-tone components of the same order and defines the nt-order **I**nter-**M**odulation **D**istortion (n > 1) in percent

$$IMD_n = \frac{\left| P(j\omega_2 - (n-1)j\omega_1) \right| + \left| P(j\omega_2 + (n-1)j\omega_1) \right|}{\left| P(j\omega_2) \right|} 100 \tag{17}$$

or in decibel

$$L_{IMD,n} = 20 \lg\left(\frac{IMD_n}{100} \right). \tag{18}$$

Summarizing all nth-intermodulation distortion gives the **T**otal **I**nter-**M**odulation **D**istortion in percent.

$$IMD_{Total} = \sqrt{\sum_{i=2}^{N} \exp_{10}(IMD_i/10)} \cdot 100 \tag{19}$$

or in decibel

$$L_{IMD,total} = 20\lg\left(\frac{IMD_{Total}}{100}\right). \tag{20}$$

In the paper two kinds of intermodulation distortion measurements are used:

1. Sweeping the Bass-Tone

   The first tone f_1 is varied from $f_s/2$ to $2f_s$ and the second tone is set at the constant frequency $f_2=10f_s$.

2. Sweeping the Voice-Tone

   The fist tone is set at a constant frequency $f_1=f_s/5$ and the second tone f_2 is varied from $7f_s$ to $20f_s$.

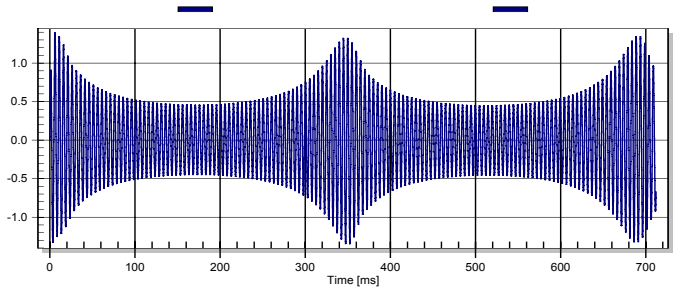

Figure 19: Amplitude modulation of a high-frequency tone by a low frequency tone caused by force factor *Bl(x)*

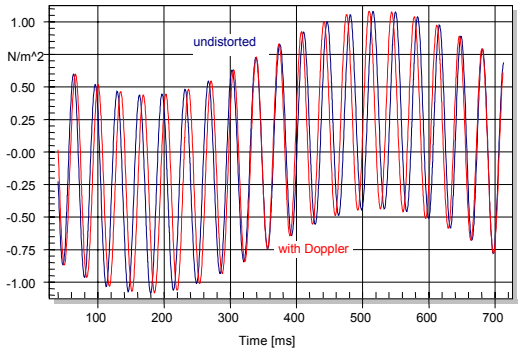

Figure 20: Phase modulation of a high-frequency tone by a low frequency tone caused by the Doppler effect

4.3.4. Separation of *FM* and *AM* Distortion

The IEC standard and other traditional intermodulation measurements exploit the amplitude of the tones in the sidebands only. The phase of the components give further information to identify the modulation mechanism:

The **A**mplitude **M**odulation (AM) causes a variation of the envelope of the first tone (carrier) according to the modulating second tone but does not affect the phase of the carrier. The parametric excitation due to the *Bl(x)* is a typical example for amplitude modulation. Figure 19 shows one period of the low frequency tone modulating the envelope of the radiated high-frequency tone.

The **F**requency **M**odulation (*FM*) does not change the envelope of the signals but changes the phase of the high frequency tone. For example, Figure 20 shows the waveforms of a radiated two-tone signal with and without Doppler effect over one period of the low frequency tone. The phase of the high frequency tone changes with the amplitude of the low frequency tone.

The intermodulation generated by an *AM*-process can be described by the **A**mplitude **M**odulation **D**istortion expressed in percent

$$AMD = \frac{\sqrt{\frac{2}{K}\sum_{k=1}^{K}\left(E[k]-\overline{E}\right)^2}}{\overline{E}} * 100 \qquad (21)$$

or in decibel

$$L_{AMD} = 20\lg\left(\frac{AMD}{100}\right) \qquad (22)$$

by using the instantaneous envelope *E[k]* and the averaged envelope

$$\overline{E} = \frac{1}{K}\sum_{k=1}^{K} E[k] \tag{23}$$

of the modulated high-frequency tone which can be calculated from complex spectrum by using the analytical signal [15].

The measures *AMD* and L_{AMD} show the contribution of amplitude modulation and can be compared with the total intermodulation measures IMD_{Total} and $L_{IMD,total}$ which consider both *FM* and *AM* distortion.

4.4. Dc-Displacement

If some of the nonlinearities have an asymmetrical shape a rectification process takes place and a dc-component X_{dc} is generated in the voice coil displacement. A dc-part can not be generated in velocity, acceleration and the corresponding sound pressure output because those time signals are derivatives of the displacement. The voice coil current is also free of a dc-component because the magnetic flux is differentiated and the back-EMF is the product of two orthogonal time signals (displacement and velocity).

5. EFFECTS OF THE CURVE SHAPE

There are some general relationships between the shape of nonlinearity and the magnitude of the low- and high-order distortion components independent on the physical context and the place of the nonlinearity in the differential equation.

The following discussion uses the Bl(x)-nonlinearity as example.

5.1. Symmetry and asymmetry

The most obvious feature of a nonlinear parameter is the symmetry of the curve. A well made loudspeaker should have a symmetrical $K_{ms}(x)$ and *Bl(x)* curve. At high positive and negative excursion the suspension will be limited by unfolded and stretched suspension material and the voice coil will leave the gap. A symmetrical curve usually produces 3rd- and other odd-order distortion components as illustrated in Table 2. No dc-displacement and other even-order distortion are generated as long as the nonlinear system behaves stable. A loudspeaker may become unstable if a motor with an equal-length configuration is combined with a soft suspension.

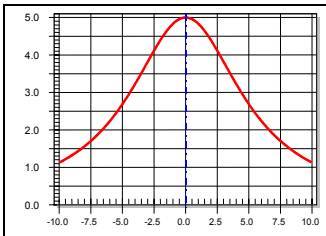 Symmetrical Nonlinearity	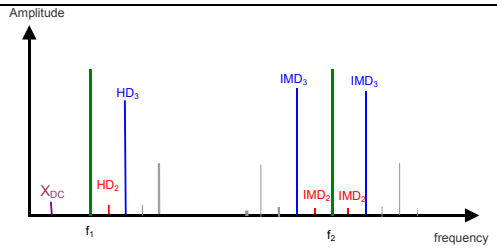 Symmetrical nonlinearity generates high 3rd-order distortion (*HD_3, IMD_3*)
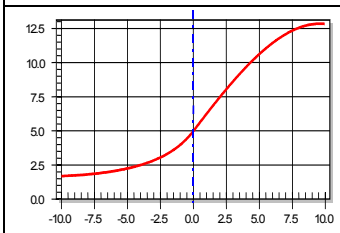 Asymmetrical Nonlinearity	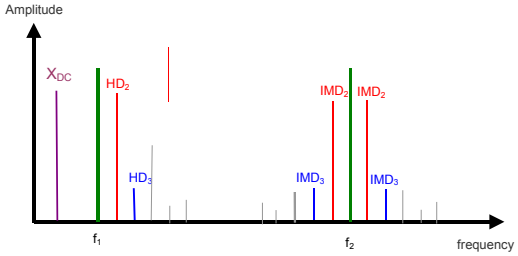 Asymmetrical nonlinearity generates high 2nd-order distortion (*IMD_2, HD_2*)

Table 2 Relationship between shape of nonlinearities and the generated odd- and even-order distortion components

Other nonlinearities such as the inductance of a driver without shorting ring, the Doppler effect and wave steepening have a distinct asymmetry and generate even-order distortion primarily. However, since the nonlinearity is usually part of a feedback loop (nonlinear differential equation) and odd-order distortion are also generated by multiplying the even-order distortion with the fundamental component.

5.2. Soft- and hard-limiting nonlinearities

Another obvious feature of the nonlinear curve shape is the steepness of the curve. Motors where coil and gap have the same length become nonlinear at relatively small displacement as shown as dashed line in Figure 5. Contrary a large voice coil overhang causes a plateau where the force factor is almost constant over a certain range as shown as solid line in Figure 5. However, when the coil leaves the gap the force factor decays at a much higher rate than the equal-length configuration. For high displacement of half the coil height (x=+-5 mm) both configurations give the same force factor value (Bl = 2.5 N/A) neglecting the influence of the fringe field. If both curves are expanded into a power series the coefficient of the quadratic term is dominant for the equal-length configuration but the overhang coil will result in a dominant higher-order coefficient.

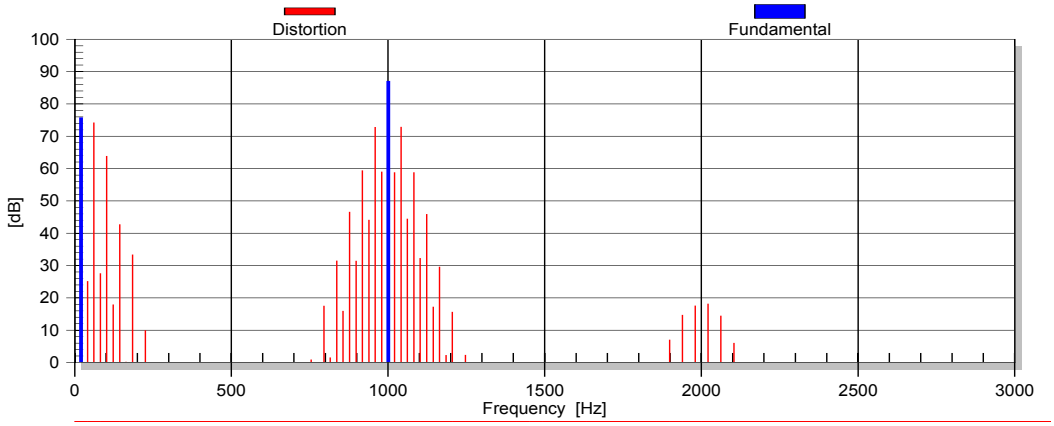

Figure 21: Spectrum of distorted two-tone stimulus in sound pressure output generated by a force factor *Bl(x)* of an equal-length coil configuration

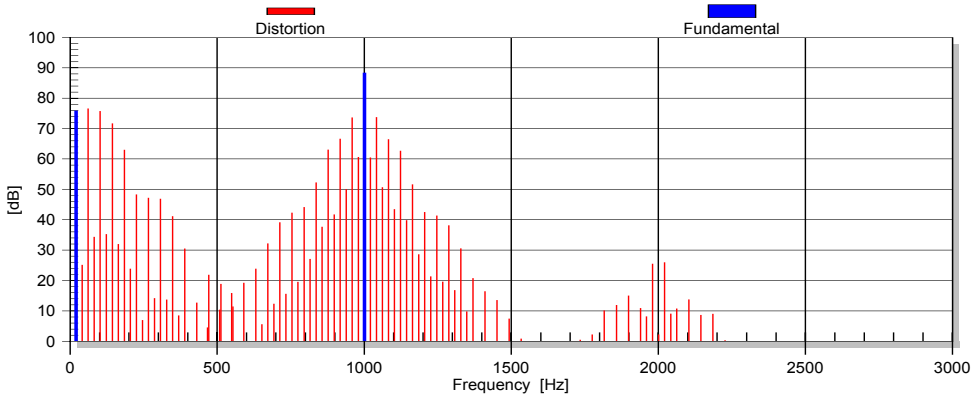

Figure 22: Spectrum of distorted two-tone stimulus in sound pressure output generated by a force factor *Bl(x)* of an overhang coil-gap configuration

The steepness of the nonlinear curve directly corresponds with the energy of the higher-order components.

Figure 21 shows the spectrum of the distorted two-tone signal caused by the force factor of the equal-length configuration. Clearly the third-order distortion is maximal and the fifth- and higher-order components decay fast. A nonlinearity with a more distinct on-set like the *Bl(x)* of an overhang coil produces larger higher-harmonics as shown in Figure 22.

While the spectra are measured at a particular voice coil displacement (x_{peak}= 5mm) it is also interesting to investigate the dependency on the displacement (which stands for the amplitude of the excitation).

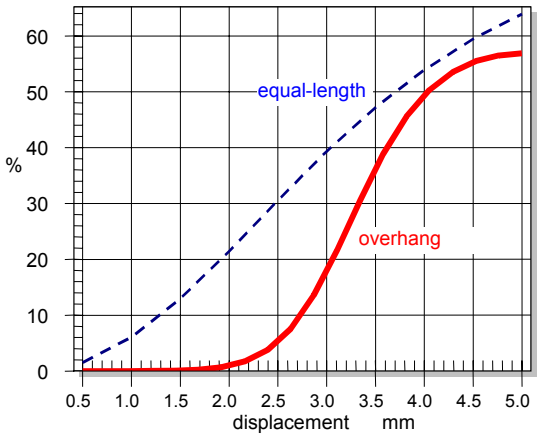

Figure 23: Total harmonic distortion (*THD*) in percent versus voice coil displacement for a motor with overhang coil (thick line) and with an equal-length configuration (dashed line).

Figure 23 shows total harmonic distortion *(THD)* for both configurations measured at the resonance frequency versus voice coil displacement *x*. Since the equal-length configuration causes an early decay, the distortion rise almost linearly with displacement. The equal-length configuration produces at x_{peak}=2.5 mm already 30 % THD but the distortion of the overhang coil are still small. However, at higher displacement the distortion of the overhang coil rise with a much higher rate to almost the same value as the equal-length configuration.

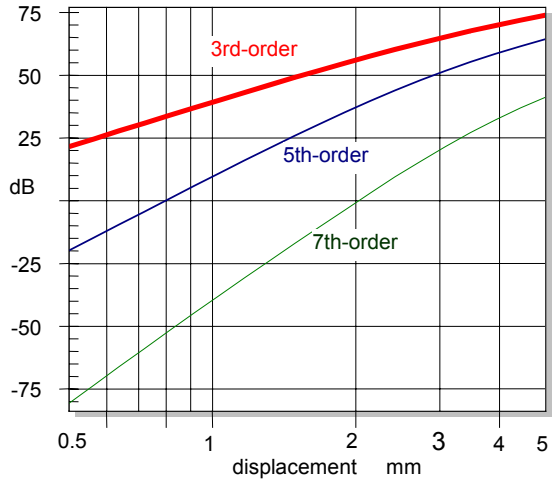

Figure 24: Amplitude of 3rd, 5th and 7th-order harmonic distortion components in sound pressure versus displacement for an equal-length configuration

It is also interesting to investigate the dependency of each component versus displacement. Figure 24 shows the 3rd-,5th- and 7th-order distortion generated by the equal-length configuration versus displacement on a double logarithmic scale. Below 2 mm all the curves are almost perfectly straight lines whose gradient rises with the order of the distortion. This is typical for a weak nonlinear system with a smooth curve shape. The third-distortion are below 5 % and the higher-order distortion are practically negligible. The large signal domain starts at 3 mm where the amplitude compression starts and all of the distortion curves rise at a smaller rate. Due to the feedback loop in the nonlinear differential equation the distortion components reduce the fundamental and disturb their own generation process. Even at 5 mm displacement the 7th-order distortion are 25 dB below the 3rd-order component.

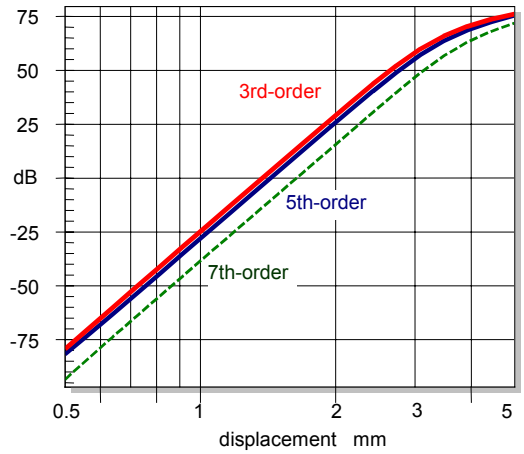

Figure 25: Amplitude of 3rd, 5th and 7th-order distortion components in sound pressure versus displacement for an overhang coil

Figure 25 reveals a complete different behavior of the overhang coil representing a hard-limiting nonlinearity. In the small signal domain all of the curves are also straight lines but rise at the same rate. Furthermore, low and higher-order give almost the same distortion level. At x_{peak}=3 mm the on-setting amplitude compression indicates the large signal behavior. Also here the distortion components stay in the same order of magnitude.

These simulations show pro and cons of the two configurations: The overhang coil gives clearly much less distortion at low and medium amplitude (below the on-set point of the hard limiting nonlinearity) while the equal-length configuration (representing a soft limiting nonlinearity) produces low-order distortion already at low amplitudes. Operating the loudspeaker in the full large signal range where the coil is half out of the gap the

overhang coil produces higher-order harmonics of larger amplitude. Since those components are located at larger distance from the fundamental components they are less masked by our auditory system and will more likely degrade the subjectively perceived sound quality.

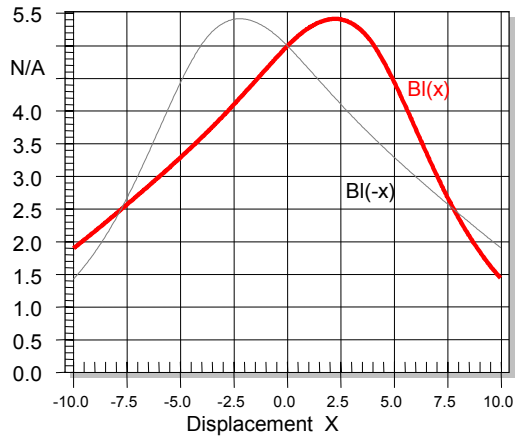

Figure 26: Twisted force factor characteristic

5.3. Twisted Curves

A third graphical feature of the curve shape is the gradual change of the asymmetry causing a twisted curve shape. For example Figure 26 shows a *Bl*-curve which has a distinct maximum at x=2.5 mm. However, the force factor decays for positive displacement at a much higher rate than on the left slope towards negative displacement. Thus, the force factor is at positive displacement of +10 mm lower than for –10 mm. Such a twisted curve shape has a characteristic effect on the distortion as shown in Figure 27.

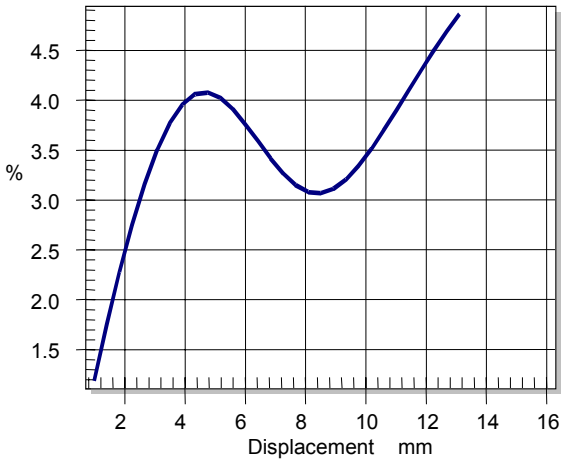

Figure 27: 2nd-order harmonic distortion versus displacement of a motor with asymmetric force factor characteristic as shown in Figure 26.

At small displacement (x < 4 mm peak) the 2nd-order distortion rise as expected with the displacement. The distortion fall for medium amplitudes (4 mm < x < 8 mm peak) and rise again at high amplitudes. Thus, if the direction of the asymmetry varies with displacement some effects can be compensated. This example shows that a distortion measurements at one amplitude level can not give a comprehensive description of the large signal behavior.

6. SYMPTOMS OF LOUDSPEAKER NONLINEARITIES

After discussing the effect of the nonlinear curve shape in general, the physical particularities of the dominant loudspeaker nonlinearities shall be investigated in greater detail. It is the goal of this chapter to find characteristic symptoms for each nonlinearity. Table 3 anticipates the result of the following discussion. The cross-symbol (X) shows measurements which provide meaningful symptoms for the particular nonlinearity. The circle-symbol (☼) marks unique symptoms which are sufficient to identify the cause of the distortion.

Nonlinearities	**SYMPTOMS GENERATED IN MONITORED STATE VARIABLE**							
	Sound Pressure				Current			Displacement
	HD	*IMD* (bass sweep)	*IMD* (voice sweep)	*AMD* (voice sweep)	*HD*	*IMD* (bass sweep)	*IMD* (voice sweep)	X_{dc}
$K_{ms}(x)$ suspension (spider +surround)	X							X*
Bl(x) electro-dynamical motor	X	X	X	X				X*
$L_e(x)$ position of coil in the gap		X	X	X		X*	X	
$L_e(i)$ "flux modulation"	X	X	X	X	X*	X*	X	
Variation of Geometry of Cone and suspension	X	X	X	X				
Young's-modulus $E(\varepsilon)$ of cone and suspension	X	X	X	X				
Flow resistance $R_A(v)$ in ports of vented enclosures	X							
Doppler Effect radiation of sound waves		X	X					
Wave Steepening sound propagation at high SPL	X		X					

* provides unique symptoms which are sufficient for the identification of the nonlinearity.

Table 3 Characteristic symptoms such as harmonic distortion (*HD*), intermodulation distortion (*IMD*), amplitude modulation distortion (*AMD*), dc-displacement (X_{dc}) of the dominant loudspeaker nonlinearities (unique symptoms are represented by ☼)

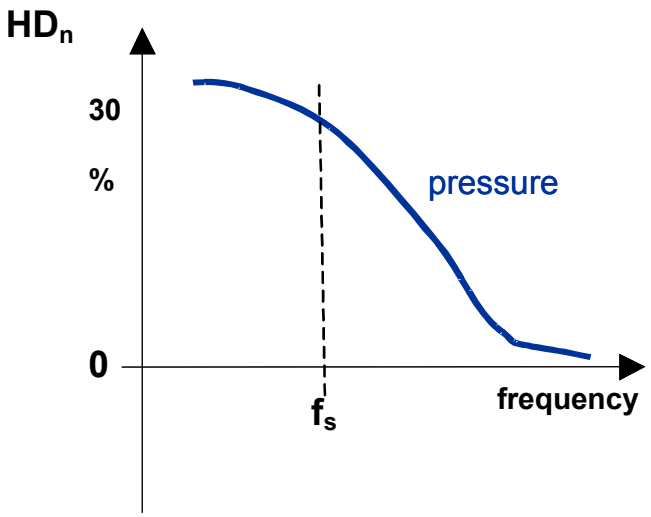

Figure 28: Characteristic frequency response of nth-order harmonic distortion caused by nonlinear stiffness $K_{ms}(x)$

6.1. Displacement varying stiffness $K_{ms}(x)$

Table 1 shows that the restoring force $F=K_{ms}(x)x$ of the suspension is a function of the displacement x only. Since displacement is a low-pass filtered signal, the multiplication of x with x will produce distortion components (both harmonic and intermodulation) which are restricted to low frequencies (for a soft limiting suspension below $5f_s$). A stimulus comprising a low and high frequency tone will not produce significant intermodulation components because the displacement of the high frequency tone is too small. Harmonic distortion measurement is a sensitive but not unique symptom of the $K_{ms}(x)$-nonlinearity as illustrated in Table 3.

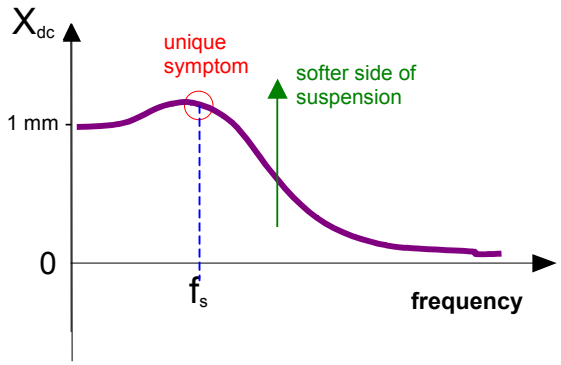

Figure 29: Frequency response of dc-displacement which is characteristic for an asymmetric $K_{ms}(x)$-nonlinearity.

If the $K_{ms}(x)$-curve is asymmetric, the generated dc displacement X_{dc} is also a characteristic symptom. Low frequencies which contribute to the ac-displacement contribute to the dc-component as shown in Figure 29. The dc-displacement $X_{dc}(f_s)$ at the resonance frequency f_s is a unique symptom for the K_{ms}-nonlinearity. As discussed in greater detail below all of the other dominant nonlinearities can not produce a significant dc-component at f_s.

The sign of the dc-part is also a valuable information. The dc-part moves the coil always towards the side where the suspension is softer. If the $K_{ms}(x)$ curve is not twisted the dc-part has always the same polarity and is independent of the amplitude and frequency of the stimulus.

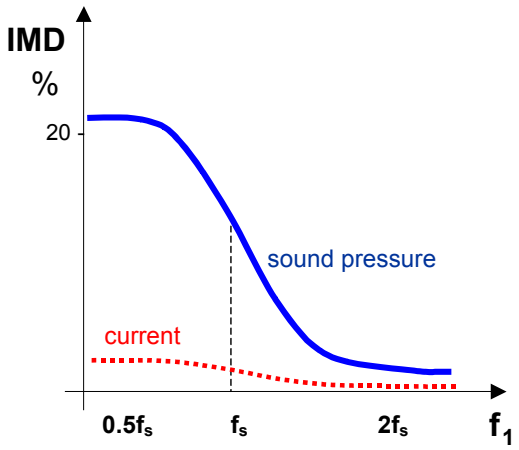

Figure 30: Frequency response of intermodulation distortion (*IMD*) in sound pressure output and input current which is characteristic for a *Bl(x)*-nonlinearity (sweeping the *bass tone)*

6.2. Displacement varying Force Factor *Bl(x)*

The *Bl(x)*-nonlinearitiy causes two effects as shown in Table 1, namely the nonlinear damping and the parameteric excitation. Both effects generate high harmonic distortion at low frequencies where displacement, current and velocity are high. The response is almost similar to Figure 28 caused by the K_{ms}-nonlinearity. Thus the harmonic distortion measurements provides no a unique symptoms to distinguish between *Bl(x)* and $K_{ms}(x)$ nonlinearity.

However, the parametric excitation produces high intermodulation distortion in the upper audio band if a first tone provides high displacement and a second tone sufficient current. Figure 30 shows a typical *IMD*- response versus frequency f_1 varied at low frequencies ($0.5f_s < f_1 < 2f_s$) while keeping the voice tone at $f_2=10f_s$. The *IMD* measured in the sound pressure output are significantly higher than in the current signal. Both curves decrease with frequency because the displacement vanishes above resonance.

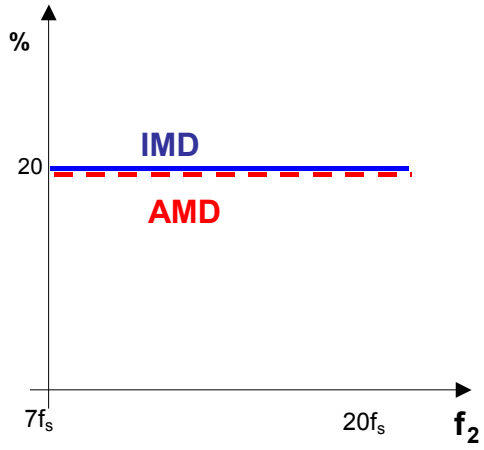

Figure 31: Frequency response of intermodulation distortion (*IMD*) and amplitude modulation distortion (*AMD*) in sound pressure output which is characteristic for *Bl(x)*-nonlinearity (sweeping the *voice tone)*

Figure 31 shows typical *IMD* and *AMD* responses measured by using the alternative sweeping technique where the bass tone is at f_1 = 10 Hz but the voice tone is varied in the audio band. Since *Bl(x)* produces amplitude modulation both measures give identical values. Both values are also independent of the frequency because the bass tone provides constant peak displacement.

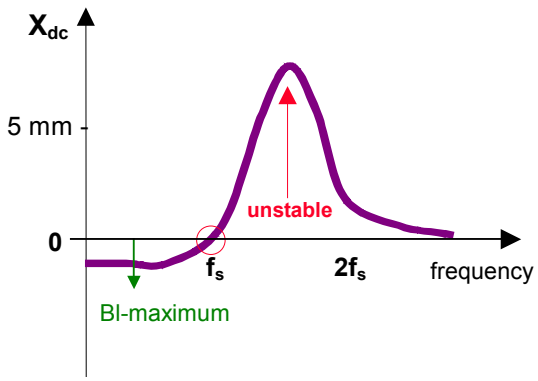

Figure 32: Frequency response of dc-displacement which is characteristic for an asymmetric *Bl(x)*-curve.

The parametric excitation also generates a dc-displacement if the *Bl(x)*-curve is asymmetrical. However, the sign of the dc-part depends on the phase of current and displacement multiplied with each other and gives the typical response shown in Figure 32.

A single tone below resonance generates a relatively small dc-part which moves the coil towards the *Bl*-maximum. This behavior may partly compensate for an offset in the coil's rest position. The dc-part vanishes at the resonance where current and displacement become 90 degree output of phase. At higher frequencies the self-centering capability turns into the opposite and the coil has the tendency to slide down on either slope of the *Bl(x)*-curve. Even in a perfectly symmetrical *Bl(x)* curve a small disturbance may initiate the coil-jump-out process. This shows that the electro-dynamical transducer is potentially unstable. However, the dc-force generated by the motor has to cope with the stiffness of the suspension at dc. Unfortunately, some suspension material have a significantly lower stiffness at dc than at resonance frequency f_s [16]. Consequently, the visco-elastic properties of the suspension material are important for the stability of the motor structure. The zero point of the dc-part ($X_{dc}=0$) at f_s is a unique symptom for the *Bl(x)*-nonlinearity. A zero point can only be produced by other nonlinearities ($L_e(x)$ and $K_{ms}(x)$) if the curve is twisted or if the dc-components of two different asymmetrical nonlinearities cancel out each other.

6.3. Displacement varying inductance $L_e(x)$

The $L_e(x)$-nonlinearity supplies distortion directly into the electrical circuit which can easily be detected in the input current. According Table 1 this nonlinearity multiplies current and displacement which are differentiated afterwards.

$L_e(x)$-nonlinearity produces relatively low harmonic distortion. At low frequencies both current and displacement are high but the differentiator attenuates the harmonics. At the resonance the current is low and at higher frequencies the displacement vanishes.

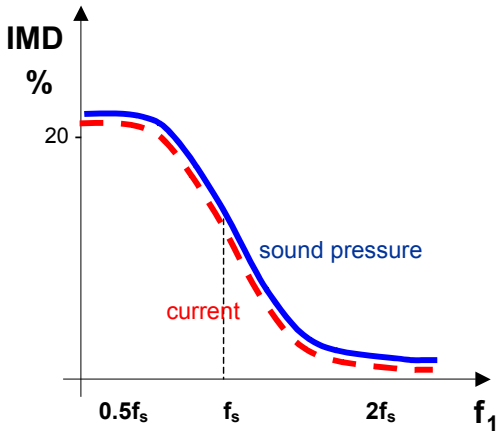

Figure 33: Frequency response of intermodulation distortion (*IMD)* in sound pressure and current which is characteristic for *L(x)*-nonlinearity (sweeping the *bass tone)*

However, a two-tone signal may activate high intermodulation distortion because the low frequency tone f_1 provides high displacement and the high frequency tone f_2 sufficient current. It is a unique feature of the $L_e(x)$-nonlinearity that the *IMD* detected in the current equal the *IMD* found in the sound pressure output. This is illustrated in Figure 33 where the bass tone is varied and the distortion decays above resonance frequency.

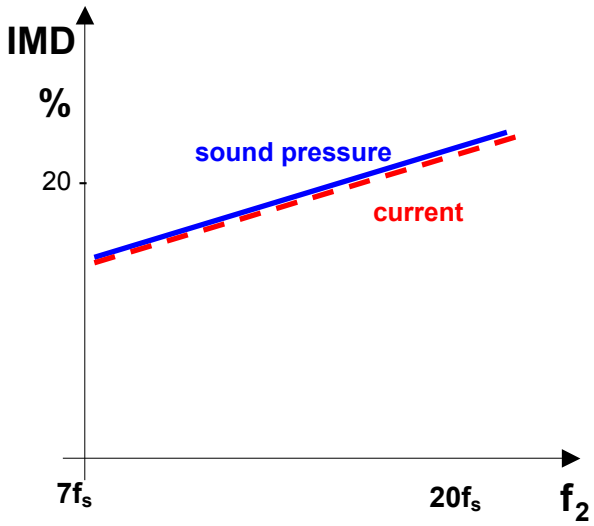

Figure 34: Frequency response of intermodulation distortion (*IMD*) and amplitude modulation distortion (*AMD*) in sound pressure output which is characteristic for $L_e(x)$-nonlinearity (sweeping the *voice tone)*

Figure 34 shows the *IMD* measured with the alternative sweeping technique where the voice tone is varied while keeping the bass tone at a constant frequency. This curve reveals the effect of the differentiator which causes an increase of about 6 dB/octave in the *IMD* and *AMD* response.

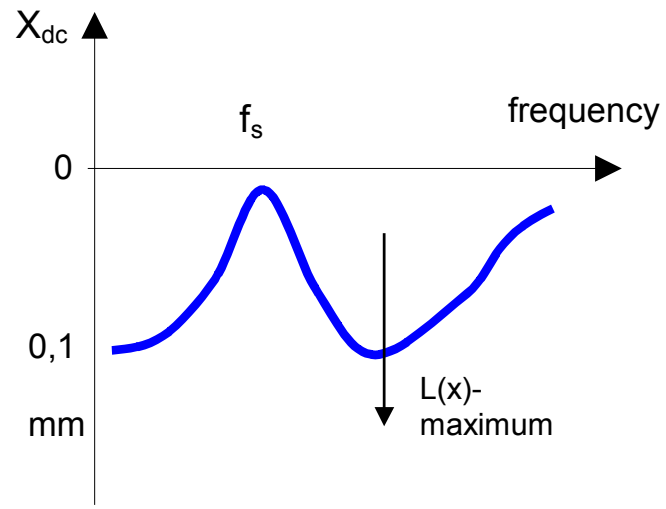

Figure 35: Frequency response of dc-displacement which is characteristic for an asymmetric $L_e(x)$-nonlinearity

The reluctance force generates a unique symptom in the dc-displacement as shown in Figure 35. Since the reluctance force is proportional to the squared input current, the force becomes minimal at the resonance frequency f_s. Furthermore, the force and resulting dc-displacement does not change the sign as long as the $L_e(x)$ has not a twisted curve shape.

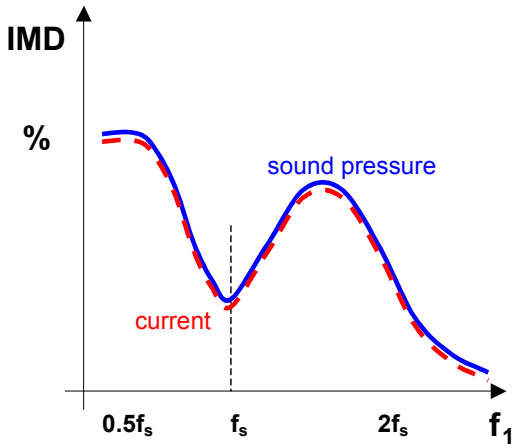

Figure 36: Frequency response of Intermodulation distortion (*IMD*) in sound pressure and current which is characteristic for current varying inductance *L(i)* (sweeping the *bass tone)*

6.4. Current varying Inductance $L_e(i)$

The variation of the permeability expressed by the current varying inductance $L_e(i)$ causes a multiplication of current signals prior to the differentiation as shown Table 1. The intermodulation distortion measurement with varying bass tone frequency reveals a unique symptom. The *IMD* response has a characteristic minimum at the resonance frequency f_s as shown in Figure 36. The *IMD* distortion and the harmonic distortion at higher frequencies measured in sound pressure and current are also identical. Contrary to the displacement varying nonlinearities ($Bl(x)$, $K_{ms}(x)$ and $L_e(x)$) this nonlinearity can also produce significant harmonic distortion (*HD*, *THD*) in the input current and sound pressure output as shown in Figure 37. Harmonics in current and sound pressure are comparable after transforming both results into the equivalent input distortion (EHD).

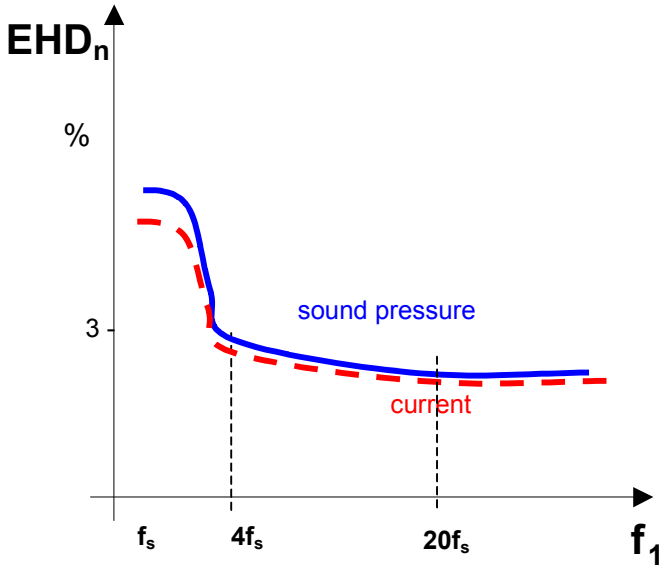

Figure 37: Frequency response of equivalent harmonic input distortion (EHD) measured in sound pressure and current which is characteristic for a current varying inductance *L(i)*

6.5. Variation of the Geometry

This mechanisms is directly related with the occurrence of break-up modes. Thus the distortion are generated at relatively high frequencies (*>10f*$_s$). The distortion can easily be measured in the acoustical output but are hardly detectable in the input current. Comparing both measurements may be helpful to separate motor nonlinearities. Maxima in the frequency response of the equivalent harmonic input distortion (*EHID*) corresponds with break-up modes of high amplitude. Narrow dips are caused by cancellation effects with other nonlinearities.

Scanning the cone and suspension surface and measure the distortion directly in the mechanical system would give deeper insight into the nonlinear process.

The intermodulation between a low and high-frequency tone are mostly amplitude modulation. The variation of the surround geometry changes the mechanical impedance at the end of the cone and has significant impact on the amplitude of particular modes.

6.6. Material nonlinearities

The variation of the Young's *E*-module produces similar symptoms as the variation of the cone and surround geometry. The measurement of harmonic distortion in the sound pressure output gives significant symptoms.

Intermodulation measurement should avoid a low frequency component because a bass tone will cause a significant deformation of the surround geometry which dominates the material nonlinearities.

6.7. Port Nonlinearity

To evaluate the performance of the port the vented loudspeaker system is excited at the port resonance frequency (Helmholtz resonance) where volume velocity *q* is maximal but the displacement of the loudspeaker minimal. The harmonic distortion are measured in the sound pressure output at 1 m distance (to get a good signal-to-noise ratio). Measurements closer at the port may be affected by air convection. To separate the effect of the port from other loudspeaker nonlinearities the displacement of the cone is also measured by using a laser system. The equivalent harmonic input distortion calculated from sound pressure signal and the displacement become comparable and the difference shows the contribution of the port. The third-order harmonic are usually dominant if the port geometry is symmetrical. Measurements of intermodulation distortion will not provide unique symptoms.

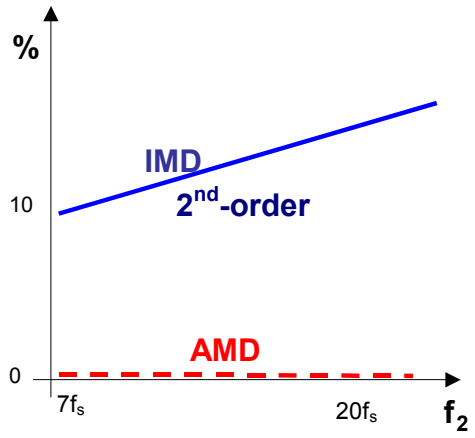

Figure 38: Frequency response of intermodulation distortion (*IMD*) and amplitude modulation distortion (*AMD*) in sound pressure output which is characteristic for the Doppler effect (sweeping the *voice tone)*

6.8. Doppler Effect

The harmonic distortion measurement is not useful for detecting the Doppler effect. A signal tone can not provide at the same time sufficient displacement and a short wavelength to produce a significant phase shift. Doppler effect can be easily detected by performing an intermodulation measurement with a varying voice tone as illustrated in Figure 38. Similar to the $L_e(x)$-nonlinearity the intermodulation rise by 6dB per octave to higher frequencies. However, the Doppler effect causes only phase modulation and the value of the amplitude modulation (*AMD*) is low. Clearly the Doppler effect can not produce any distortion in the displacement and in the input current.

6.9. *Wave Steepening*

The nonlinear sound propagation is related with the multiplication of sound pressure components. Thus this nonlinearity produces not only intermodulation but also significant harmonics. This is unique symptom to distinguish Doppler effect from wave steeping. The 2^{nd}-order distortion rise by 6dB per octave while the 3^{rd}-order distortion usually rise at a higher rate because they are generated from the 2^{nd}-order components by an additional multiplication and differentiation in following horn sections [8] .

.

7. PRACTICAL DIAGNOSTIC

The interaction and superposition of the different effects are now discussed on real three loudspeakers:

7.1. Speaker 1 with Coil offset

The first loudspeaker is a 6 inch woofer intended for high quality consumer application. The force factor characteristic *Bl(x)* as shown in Figure 39 reveals a distinct plateau region corresponding with a voice coil overhang of about 6 mm. .

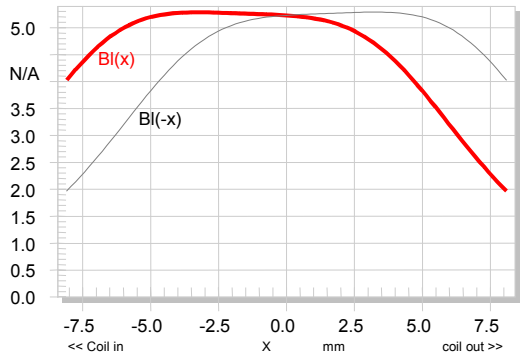

Figure 39: Force factor *Bl(x)* versus displacement of speaker 1 (dashed curve shows the mirrored *Bl(-x)*-characteristic)

The optimum rest position of the voice coil can be found by investigating the symmetry of the *Bl*-characteristic in Figure 40. Assuming a sinusoidal displacement of given *amplitude*, the coil will not see the same *Bl*-values at positive and negative peak displacement if the curve is asymmetric. By shifting the coil (*offset)* to the *symmetry point* (red dashed line in Figure 40) the same Bl-values at positive and negative peak values may be accomplished for a particular amplitude. If the symmetry point is independent of the amplitude then the asymmetry can completely be compensated by a constant voice coil shift. However, usually a compromise is required as in the example shown in Figure 40 where the symmetry point varies from –3 mm at low amplitudes to –2 mm at higher amplitudes. The *symmetry region* (grey area) shows where a potential offset for a given amplitude generates small asymmetrical variation (< 5 %) which are acceptable. At small amplitudes where the Bl(x)-curve has the plateau the symmetry region is wide indicating that the position of the overhang coil is not critical here. For larger amplitudes the voice coil has to be shifted by a negative offset (about -2 mm) that the coil leaves the gap symmetrically.

The rest position of the voice coil in the gap is optimal if the dotted line representing the rest position (offset=0) is in the symmetry region (grey area). If this is not the case the symmetry point gives some indication for a voice coil shift.

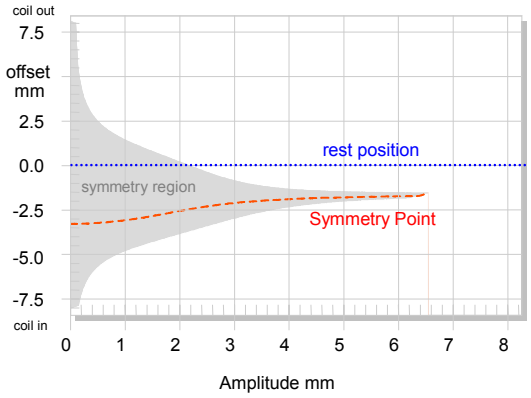

Figure 40: Symmetry point (red dashed line) and symmetry region (grey area) reveal an offset in the coil's rest position of speaker 1.

The stiffness curve shown in Figure 41 has also a small asymmetry and $K_{ms}(x)$ increases for negative excursions to twice the value found at positive values. After removing 80 % of the surround material the measured stiffness of the remaining spider was almost symmetrical.

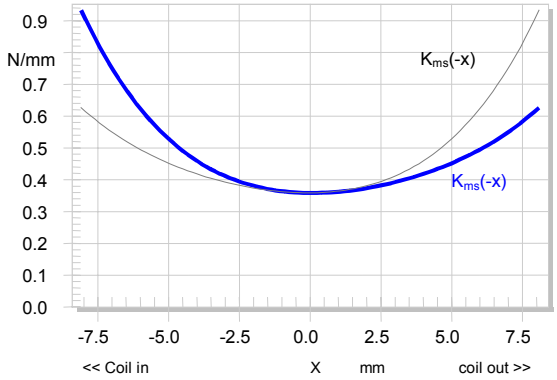

Figure 41: Stiffness $K_{ms}(x)$ versus displacement x of speaker 1 (dashed curve shows mirrored $K_{ms}(-x)$-characteristic)

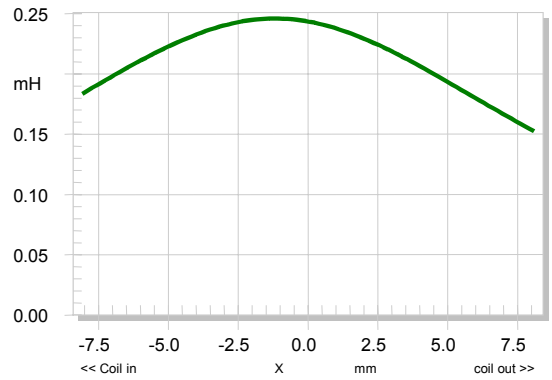

Figure 42: Inductance $L_e(x)$ versus displacement x of speaker 1

Figure 42 shows an almost symmetrical shape of the $L_e(x)$ which is not typical for a driver. The missing increase at negative displacement indicates that a shorting ring is used below the gap. The remaining maximum of inductance at x=0 may be reduced by placing an additional cap on the pole piece. However, the total inductance value is already small (compared with the R_e= 3.5 Ohm) and will not produce significant variation of the input impedance.

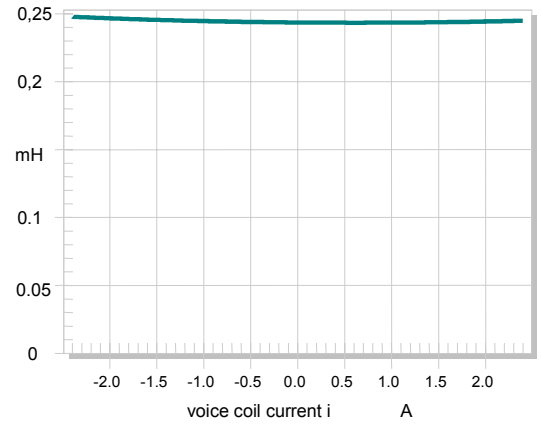

Figure 43: Inductance $L_e(i)$ versus current i of speaker 1

The variation of the voice coil inductance $L_e(i)$ as shown in Figure 43 shows that the permeability of the magnetic path is almost constant. Here the permanent field generated by the magnet is much higher than the ac field generated by the coil.

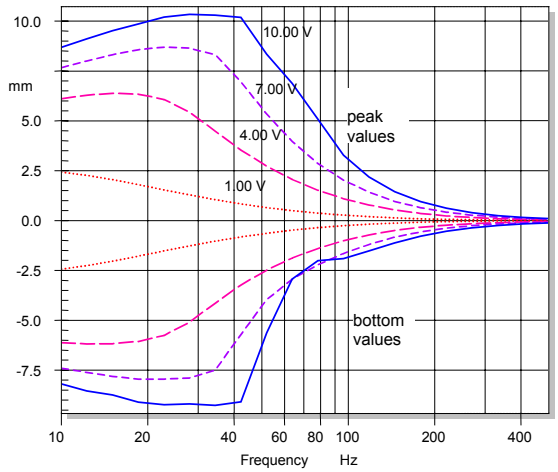

Figure 44: Peak and bottom value of voice coil displacement of speaker 1 versus frequency measured at four voltages

Figure 44 shows the peak and bottom of the voice coil displacement measured at four different voltages by a laser displacement meter. The shape of the curves varies with the input voltage. For *U=1V* the maximum of the displacement is far below resonance due to the high electrical damping and the low total loss factor Q_{ts} of the driver. However, at high voltages the electrical damping decreases (with $1/Bl(x)^2$) and the Q_{ts} becomes greater than 1. At frequencies shortly above resonance the bottom value stagnates at –2.5 mm while the peak values rise rapidly with the input voltage. This corresponds with a dc-part generated in the displacement. This is investigated in Figure 45 in greater detail.

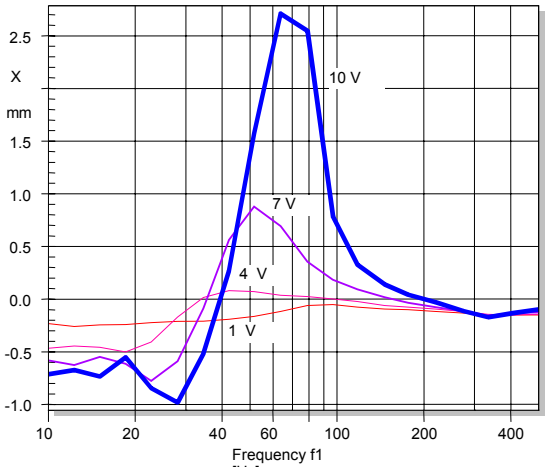

Figure 45: dc-displacement of speaker 1 measured versus frequency and at four voltages

The sign of the dc part changes at the resonance frequency f_s =*35 Hz*. For frequencies below f_s the dc part is about -0.5 mm and stays almost constant for high amplitudes of the ac signal. Here the asymmetry of *Bl(x)* generates a dc-force which moves the coil towards the *Bl*-maximum. At frequencies above f_s the consequences of the voice coil offset become obvious. The dc part becomes positive and rises quickly with amplitude (*coil jump-out effect*). The asymmetry of the stiffness $K_{ms}(x)$ as shown in Figure 41 generates a positive contribution to the dc-part and the inductance $L_e(x)$ a negative dc. However, both parts are negligible in comparison to the dc-part generated by *Bl(x).*

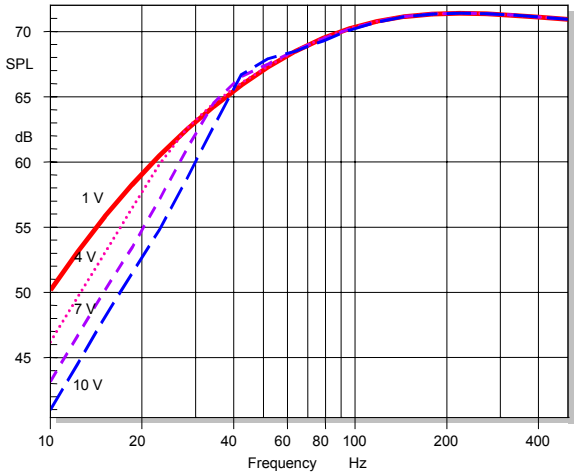

Figure 46: Sound pressure response $P_r(f, U_i)$ measured at four voltages (3 V increments) which are referred to U_i=*1 V* to reveal the amplitude compression of the fundamental in speaker 1

Figure 46 shows the frequency response of the fundamental in the sound pressure output measured at four voltages but referred to the measurement in the small signal domain (U_1=1V) according Eq. (1). Since the increase of the voltage is compensated this representation shows the power compression directly. At higher frequencies where the displacement becomes small there is no compression and the sensitivity stays constant. If the measurement time would be extended the heating of the coil would cause an additional amplitude compression (thermal effect). At low frequencies the SPL reduces by 8 dB due to the nonlinear effects. At the resonance the vanishing electrical damping causes a negative compression and the loudspeaker produces more output.

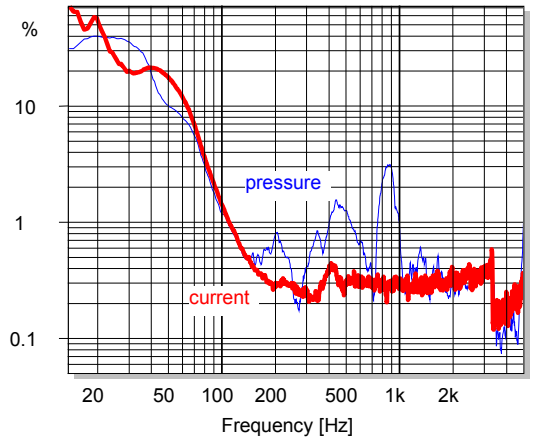

Figure 47: Equivalent total harmonic input distortion (*ETHD*) measured in the sound pressure output (thin curve) and in the voice coil current (thick curve) of speaker 1

The displacement varying force factor *Bl(x)* and stiffness $K_{ms}(x)$ generate high total harmonic distortion in the sound pressure output and in the voice coil current. To compare both signals the concept of equivalent input distortion according Eq. (8) is used. The distortion components measured in sound pressure output and current are transformed to the input (which is a voltage for a normal amplifier with low output impedance) and are presented in Figure 47 as thin and thick curve, respectively. At higher frequencies (f > 200 Hz) the distortion in the current are very low (less than 0.5 %) and are caused by the $L_e(i)$-nonlinearity. The other nonlinearities (*Bl(x),* $L_e(x)$ and $K_{ms}(x)$) are displacement depending and can not generate significant harmonic distortion. At particular frequencies e.g. 400 Hz and 800 Hz, nonlinearities in the mechanical domain (cone break-ups) produce additional distortion which interfere with the distortion found in the current. Cancellation of the two distortion components only occurs at 250 Hz but both parts usually increase the total distortion at other frequencies.

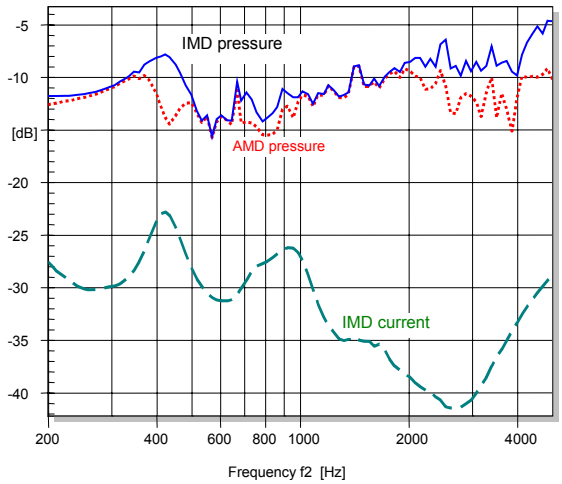

Figure 48: Total intermodulation distortion (IMD_{Total}) of speaker 1 measured in sound pressure and in voice coil current and amplitude modulation distortion (*AMD*) in the sound pressure versus frequency f_2 of the voice tone *(*constant bass tone *at* f_1*=10 Hz)*

Figure 48 shows the intermodulation distortion measured with a two-tone stimulus comprising a voice tone with variable frequency f_2 and a bass tone at fixed frequency f_1=10 Hz. The total intermodulation IMD_{total}, measured in the sound pressure output and shown as thin line, are 20 dB higher than the intermodulation found in the input current which are shown as dashed line. Thus the intermodulation caused by $L_e(x)$ and $L_e(i)$ are almost negligible compared with the contribution of the other nonlinearities.

Figure 48 also shows that the intermodulation distortion below 2kHz are caused by amplitude modulation (*AM*). For frequencies below 400 Hz the *AMD and IMD*-values are almost constant which is typical for the *Bl(x)*-nonlinearity as illustrated in Figure 31. At 400 Hz the cone performs the first partial vibration which is modulated by the varying surround geometry. Above 2 kHz the rising distortion are generated by frequency modulation.

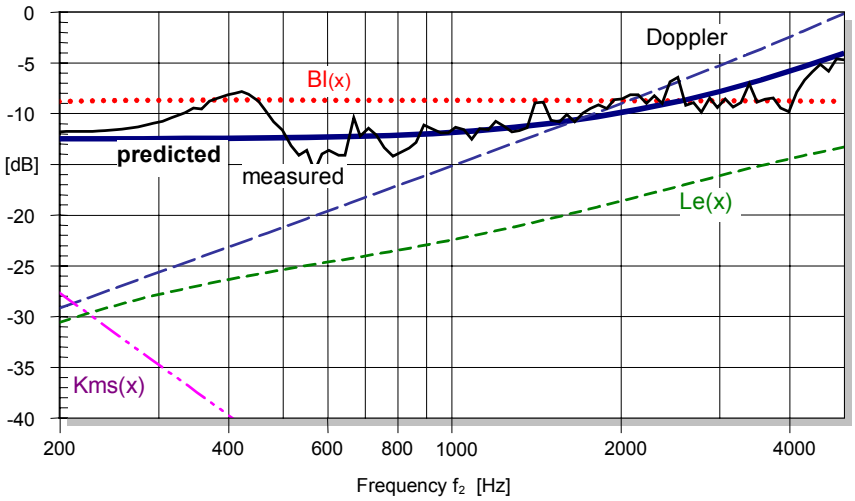

Figure 49: Measured and predicted intermodulation distortion (IMD_{total}) of speaker 1 compared with the contribution of each nonlinearity (sweeping the *voice tone)*

Further inside in the generation of the intermodulation gives the simulation tool (SIM2) of the Distortion Analyzer [19] where the total intermodulation can be predicted and the contribution of each nonlinearity can be investigated systematically.

The predicted and measured curves as shown in Figure 49 agree very well. The nonlinear cone vibration is not considered in the model but can easily separated from the motor and suspension nonlinearities. Considering the contribution of the *Bl(x)* only and switching off all of the remaining nonlinearities ($K_{ms}(x)$=const., $L_e(x,i)$=const., …) the calculated *IMD* distortion are presented as dotted curve. This curve is constant according to the theoretical shape presented in Figure 31 and is in the same order of magnitude as the predicted curve considering all nonlinearities. The distortion below 2kHz can significantly be reduced by shifting the rest position of the coil 1.5 mm to the back-plate. Above 2kHz the Doppler effect becomes dominant and produces significant phase modulation, shown as dashed line in Figure 34. However, phase modulation has less impact on the perceived sound quality than amplitude modulation which are perceived as an unpleasant roughness in the reproduced signal.

The predicted intermodulation generated by $L_e(x)$ correspond with the small values found in the input current in Figure 48 .

The low *IMD* values of the stiffness $K_{ms}(x)$ correspond with Table 3 showing that intermodulation distortion is not a significant symptom of the suspension nonlinearity.

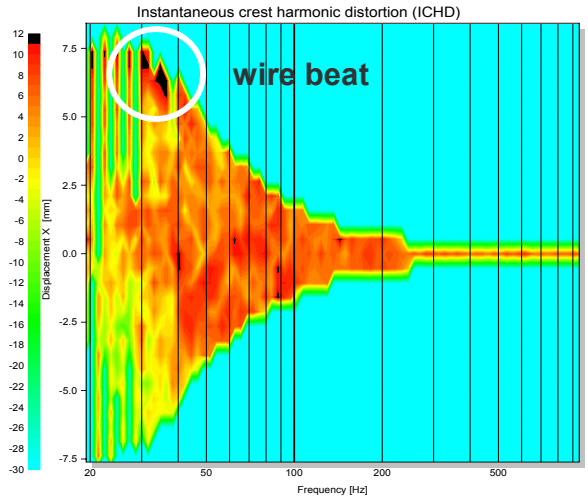

Figure 50: Instantaneous crest factor of harmonic distortion (color coded) plotted versus frequency and voice coil displacement

Finally the loudspeaker is checked for transient and impulsive distortion which have a high peak value but a relatively low *rms*-value. Figure 50 shows the instantaneous crest factor *ICHD* which is coded by the color and displayed versus frequency (x-axis) and displacement (y-axis). Below 7 mm the crest factor of harmonic distortion stays below 10 dB (blue to red) which is typical for regular nonlinearities in the motor, suspension or cone. However, at high positive displacement occurring at low frequencies ($f < 40$ Hz) the crest factor exceeds 10 dB (becoming black) which indicates a nonlinear mechanism producing short clicks at the particular coil position. Further examination of the drivers revealed that the wires beat the cone at this point.

7.2. Speaker with Suspension problem

Loudspeaker 2 is a 5 inch woofer which is also intended for consumer application.

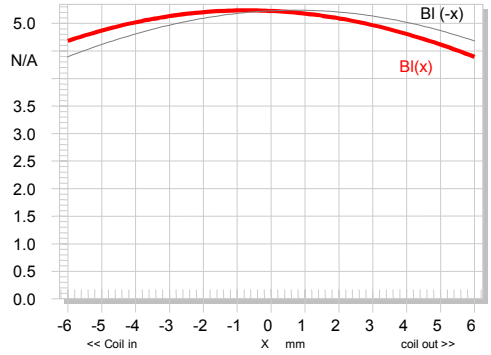

Figure 51: Force factor *Bl(x)* versus displacement of speaker 2 (thin curve shows mirrored *Bl(-x)*-characteristic)

The force factor *Bl(x)* shown in Figure 51 is relatively linear by using a high coil overhang. The curve has no plateau but a gradual decay because the fringe field outside the gap is much higher than in speaker 1.

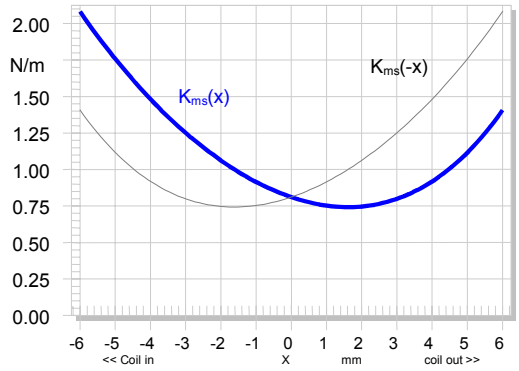

Figure 52: Stiffness $K_{ms}(x)$ versus displacement x of speaker 2 (thin curve shows mirrored $K_{ms}(-x)$-characteristic)

The stiffness curve in Figure 52 has a severe asymmetry. This is caused by the spider because a similar curve has been found in a second measurement after removing 80 % of the surround material.

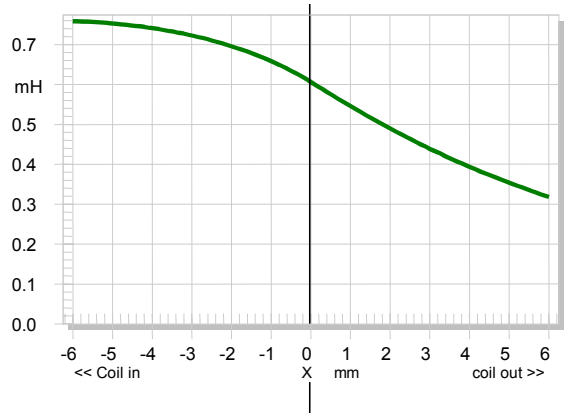

Figure 53: Inductance $L_e(x)$ versus displacement x of speaker 2

The inductance $L_e(x)$ is also asymmetric and rises for negative excursion of the coil to the back-plate. This is typical for a motor without any shorting material. While the inductance $L_e(x)$ versus displacement varies by 100 % the inductance $L_e(i)$ versus input current i in Figure 54 varies only by 10 %.

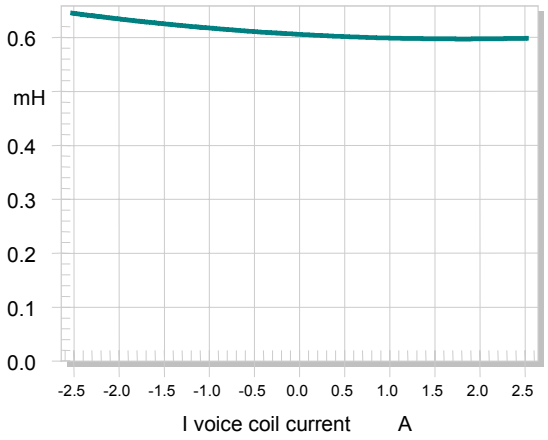

Figure 54: Inductance $L_e(i)$ versus current i of loudspeaker 2

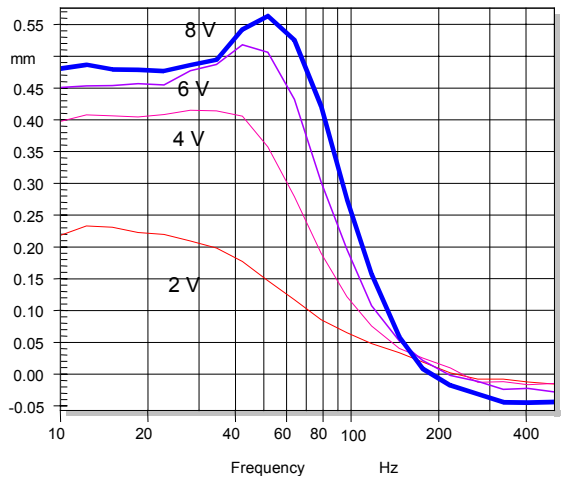

Figure 55: dc-displacement versus frequency measured at four different voltages of loudspeaker 2

The measured dc-displacement as shown in Figure 55 agrees with the asymmetries found in the nonlinear parameters. The asymmetric stiffness generates a positive displacement because the suspension is much softer for positive than negative displacement. The dc-displacement becomes maximal at the resonance frequency where the amplitude of the current is minimal and the other nonlinearities give a smaller contribution to the dc-part. At higher frequencies the stiffness asymmetry can not produce a significant dc-part because the displacement is small. Only the reluctance force generates a small negative dc-displacement and moves the coil in negative direction where the inductance $L_e(x)$ becomes higher.

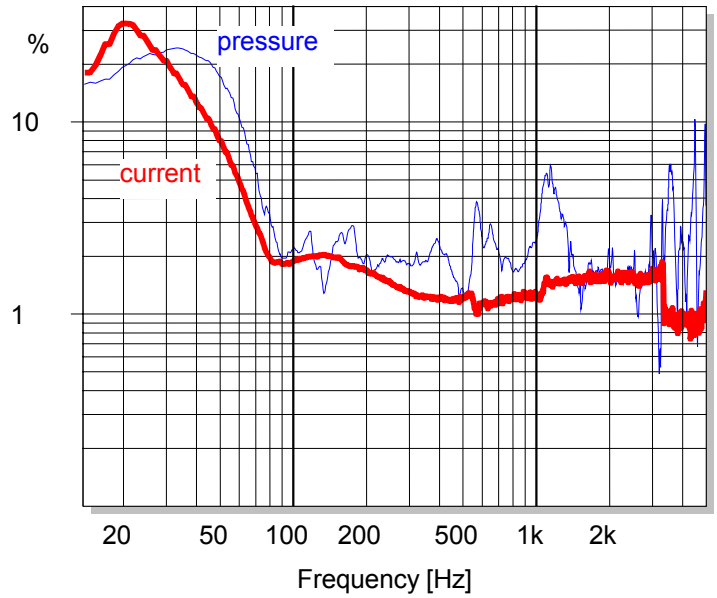

Figure 56: Equivalent total harmonic input distortion *(ETHD)* measured in the sound pressure output (thin curve) and in the voice coil current (thick curve) of loudspeaker 2

Figure 56 compares the harmonic distortion found in the input current and in the sound pressure output. At the resonance frequency and below most of the harmonic distortion found in current and sound pressure are caused by the nonlinear suspension. For frequencies above 80 Hz the nonlinear inductance $L_e(i)$ of Figure 54 generates 1 .. 2 % already in the input current. The distortion measured in the sound pressure response show interferences with the other displacement varying nonlinearities ($Bl(x)$, $L_e(x)$ and $K_{ms}(x)$) below 1000 Hz and interferences with nonlinear cone vibration at higher frequencies.

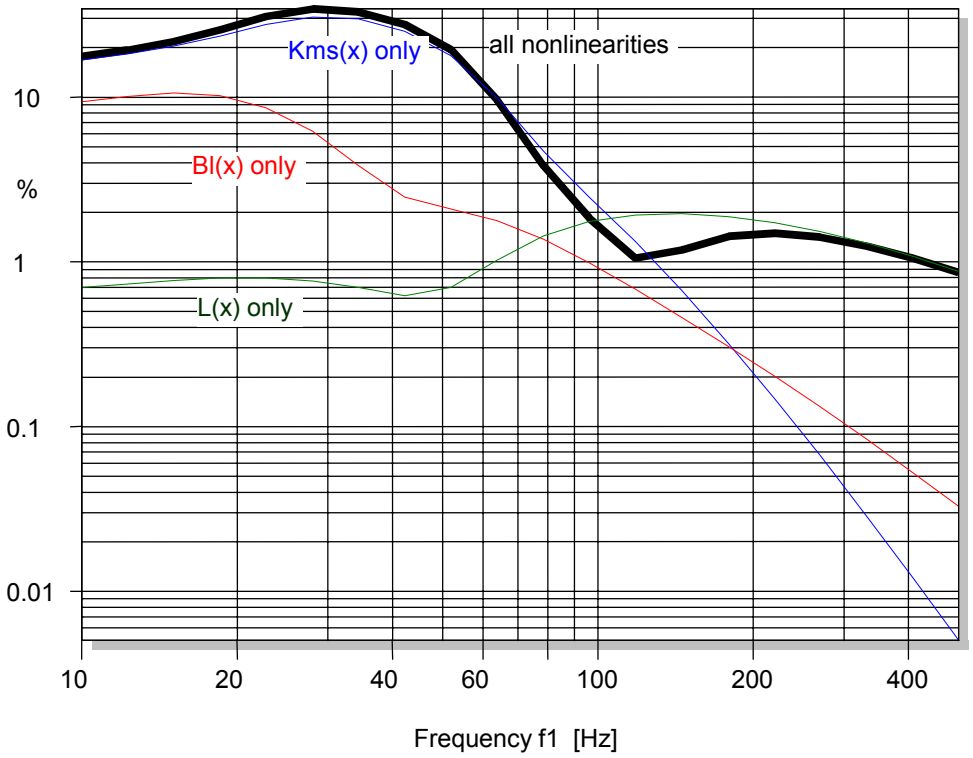

Figure 57: Equivalent total harmonic input distortion predicted by using all nonlinearities (solid curve) and in the sound pressure output (thin curve) and in the voice coil current (thick curve) of loudspeaker 2.

The identified nonlinear parameters allow to investigate the contribution of each nonlinearity in greater detail. Figure 57 shows that the stiffness $K_{ms}(x)$ is the dominant cause for the *ETHD*. The force factor *Bl(x)* produces only 10 % distortion and the inductance $L_e(x)$ produces 1 -2 %.

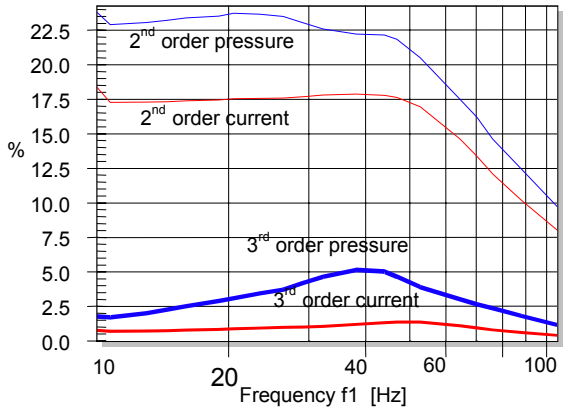

Figure 58: 2nd-order and 3rd-order intermodulation distortion measured in voice coil current and sound pressure output of loudspeaker 2 (varying bass tone, f_2=500 Hz)

Figure 58 reveals high 2nd-order intermodulation distortion $IMD_2 \approx 20$ % which is caused by the $L_e(x)$-nonlinearity because almost the same values are found in current and pressure and there is no dip at resonance frequency f_s. Due to the asymmetrical shape of $L_e(x)$ the 2nd-order component IMD_2 is much higher than the 3rd-order component IMD_3.

7.3. Loudspeaker 3 with flux modulation

Loudspeaker 3 is a 12 inch speaker intended for automotive application. Figure 59 reveals a very symmetrical $Bl(x)$ characteristic which is almost constant up to 15 mm peak value.

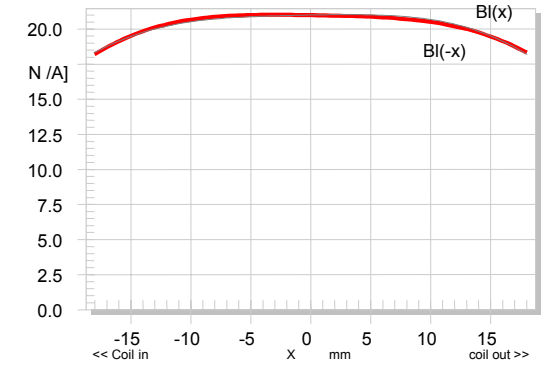

Figure 59: Force factor $Bl(x)$ versus displacement of loudspeaker 3 (thin curve shows mirrored $Bl(-x)$-characteristic)

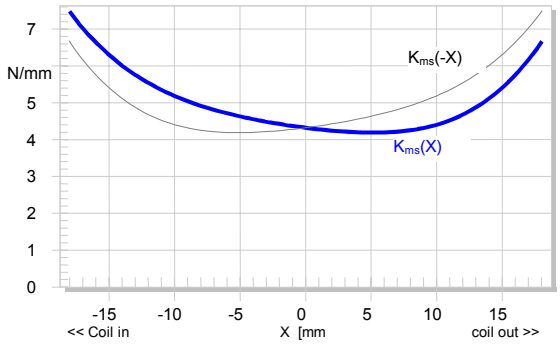

Figure 60: Stiffness $K_{ms}(x)$ versus displacement x of loudspeaker 3 (thin curve shows mirrored $K_{ms}(-x)$-characteristic)

The stiffness $K_{ms}(x)$ of the suspension as shown in Figure 60 is also almost symmetrical. The surround made of thick rubber material causes a minor asymmetry. However, the voice coil inductance varies significantly with displacement and current as shown in Figure 61 and Figure 62, respectively.

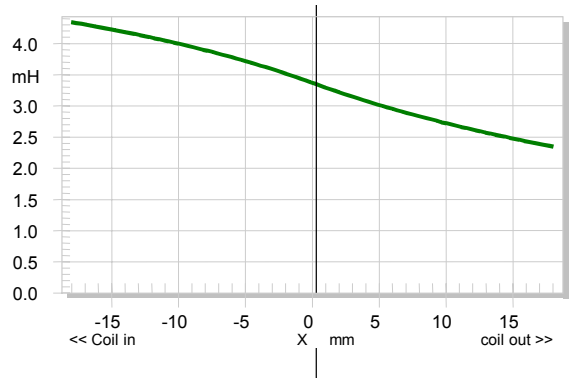

Figure 61: Inductance $L_e(x)$ versus displacement x of loudspeaker 3

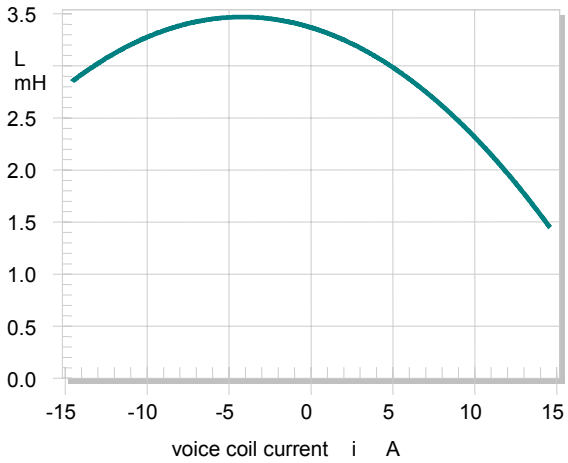

Figure 62: Inductance $L_e(i)$ versus current i of loudspeaker 3

The asymmetrical shape is typical for a motor without any shorting material. The inductance with 3.5 mH dominates the electrical input impedance at higher frequencies. During the large signal parameter measurement (LSI) the peak value of current and displacement exceeded 15 ampere and 18 mm, respectively, which cause significant variations of electrical input impedance at higher frequencies. The $L_e(x)$ is more asymmetric than the $L_e(i)$ characteristic.

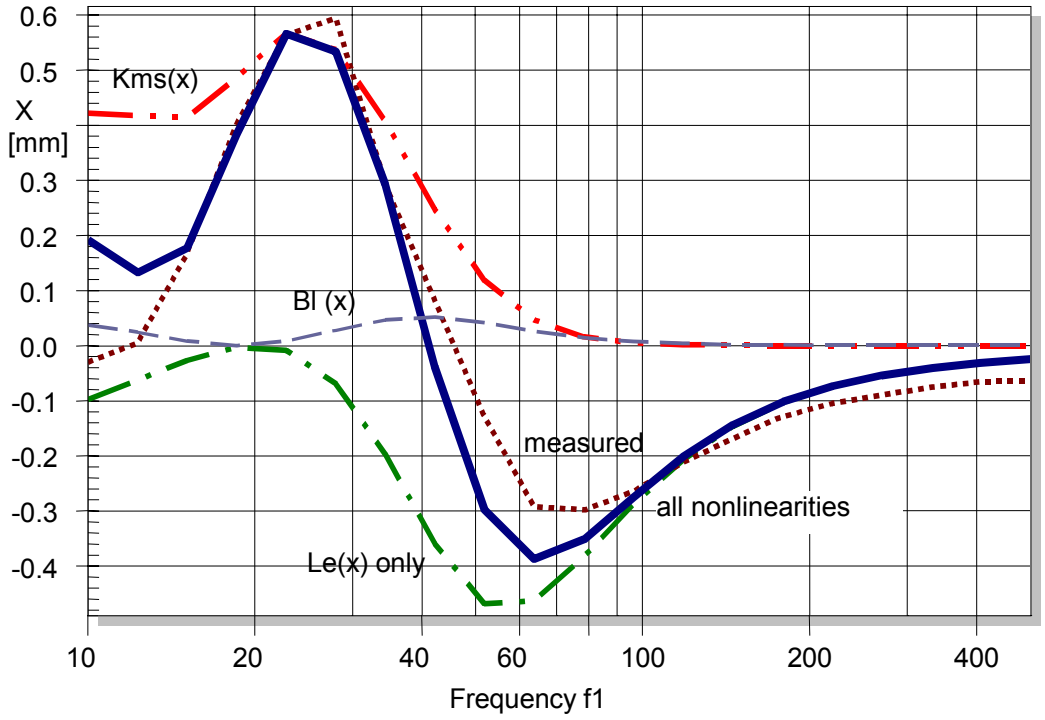

Figure 63: dc-displacement versus frequency measured (dotted line) and predicted by considering all nonlinearities (thick line) and the contribution of each nonlinearity *Bl(x),* $K_{ms}(x)$ and $L_e(x)$ of loudspeaker 3

Figure 63 shows the frequency response of the dc-displacement measured by a sensor and predicted by using the large signal parameters in the simulation software (SIM) [20]). At the resonance frequency of 25 Hz the positive dc-part of 0.6 mm is caused by the suspension which is softer for positive than for negative displacement as shown in Figure 60. The symmetrical *Bl(x)*-characteristic generates almost no dc-part. However, the asymmetric inductance $L_e(x)$ in Figure 61 generates a negative dc-part below and above f_s. At very low frequencies (10 Hz) the negative dc part of the inductance reduces the positive dc-part generated by the suspension. At higher frequencies (80 Hz) where the current becomes high again but the displacement is already small the reluctance force dominates the total dc-displacement. The zero point (X_{dc}=0) at 50 Hz is not generated by an asymmetric *Bl(x)* but caused by the interaction of two asymmetrical nonlinearities.

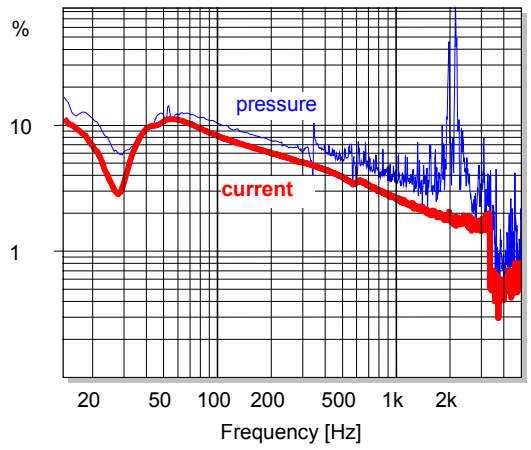

Figure 64: Equivalent total harmonic input distortion (*ETHD*) measured in the sound pressure output (thin curve) and in the voice coil current (thick curve) of loudspeaker 3

The total harmonic distortion measured in sound pressure output and current input are presented as equivalent input distortion *ETHD* in Figure 64. The high inductance nonlinearity $L_e(i)$ generates already high distortion in the input current (10% at 50 Hz) which dominates the sound pressure output. Only at 2 kHz the cone exhibits nonlinear vibration but this frequency is far beyond the intended working range of the automotive subwoofer.

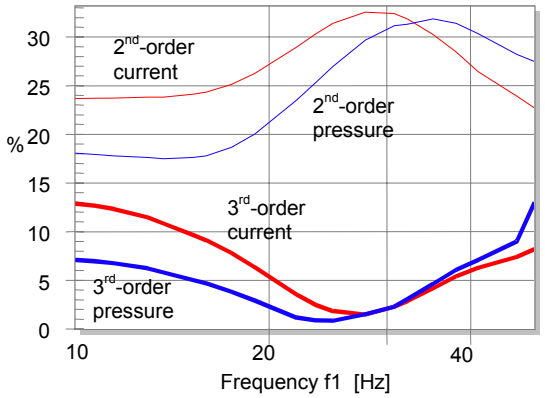

Figure 65: 2nd-order and 3rd-order intermodulation *IMD* in measured in voice coil current and sound pressure output of loudspeaker 3 (varied bass tone, f_2= 300 Hz)

The intermodulation between a bass tone at variable frequency f_1 and the voice tone at fixed frequency f_2= 300 Hz is shown in Figure 65. Like the harmonic distortion the intermodulation in current and sound pressure output is in the same order of magnitude.

According to Table 3 this is a characteristic symptom of both inductance nonlinearities $L_e(x)$ and $L_e(i)$. The 2nd-order intermodulation IMD_2 has a maximum at the resonance frequency which is typical for $L_e(x)$-nonlinearity varying with displacement. The 3rd-order distortion IMD_3 has a dip at the resonance frequency f_s which is the characteristic symptom for the $L_e(i)$-nonlinearity because the current becomes minimal there.

Loudspeaker 3 is a example of a speaker which is optimized for linear $Bl(x)$ and $K_{ms}(x)$ characteristic by using a long voice coil, a carefully designed magnetic path and a two-spider suspension. Despite the development effort, final cost and weight of the product the driver produces a highly distorted output due to the neglected $L_e(x)$ and $L_e(i)$-nonlinearities. Applying some means for shorting the ac-field can improve loudspeaker 3 significantly.

8. CONCLUSION

In the last 20 years significant progress has been made in understanding the large signal behavior of loudspeakers.

Reliable models have been developed for displacement and current varying nonlinearities in the motor and suspension system. The nonlinear parameters $Bl(x)$, $L_e(x)$, $K_{ms}(x)$ and $L_e(i)$ can be measured on loudspeakers, headphones, micro-speakers and other transducers with and without enclosure dynamically. Finite element analysis (FEA) can also be used to simulate those parameters from geometry and material parameters. The large signal model and the identified parameters allow numerical prediction of the nonlinear symptoms at high precision.

This opens the way for a new kind of loudspeaker diagnostic:

- The nonlinear parameters are easy to interpret and reveal the physical causes almost directly.
- The effect of each nonlinearity can be investigated separately and the causes for signal distortion, instabilities, compression and other nonlinear symptoms can be found.
- Design choices can easily be evaluated and the loudspeaker optimized with respect to size, weight, cost and performance

The knowledge from theory and practical application gives a new view on the general distortion measurements and shows how to make such measurements more comprehensive, time-effective, critical and easier to interpret. The most important points are:

- Nonlinear distortion measurements should be performed at different amplitude levels.

- Harmonic distortion measurements assess particular symptoms (HD_n, *THD, EID, ICHD,* …) of the loudspeaker. However, using a single tone as stimulus is not sufficient to describe the large signal performance comprehensively and to identify all loudspeaker nonlinearities.

- The stimulus should contains at least two tones at the same time to measure intermodulation distortion which are generated by the multiplication of two different state signals (e.g. displacement and current). The frequency of the tones and the sweeping techniques are critical to get results which are easy to explain. The paper suggests two techniques (sweeping the bass or the voice tone while keeping the other tone at a constant frequency)

- A stimulus with a large number of excitation tones (multi-tone testing [17]) is a good way for a fast overall check as required in QC application. However, the distortion component depends on phase and amplitude of the fundamental tones. Standardization of the stimulus is required to produce comparable results. The generated distortion pattern is a "fingerprint" of the nonlinearities which is difficult to interpret and gives no direct clues on the physical causes.

- The dc-displacement is a very informative symptom. It gives unique clues to identify the particular causes and to estimate approximately the asymmetry of motor and suspension nonlinearities.

- The amplitude compression of the fundamental and distortion components is also a symptom of loudspeaker nonlinarities. However, it gives no detailed information on the physical cause.

- The calculation of Equivalent Input Distortion (EID) is a very useful way of post-processing the measured distortion. It suppresses the influence of the linear transfer path (mechanical vibration, radiation, propagation, room, sensor) and simplifies the interpretation of the distortion responses. In this way distortion measured in displacement, current and sound pressure can easily be compared. This gives valuable clues for separating motor- and cone nonlinearities.

- The crest factor of harmonic distortion (*ICHD*) describes the smoothness of the nonlinearity. It exploits the phase information of higher-order harmonics and indicates transient, impulsive distortion caused by loudspeaker defects (e.g. rub & buzz) or extremely hard limiting nonlinearities.

These conclusions lead to a suite of objective measurements which can be accomplished in a few minutes. These measurements give a much more

comprehensive picture of the large signal performance than a traditional harmonic distortion measurement. The results can be summarized in a small set of data which is easy to interpret as demonstrated on three loudspeaker examples in this paper. Table 1 and 3, give a short summary on the dominant nonlinearities and characteristic symptoms, respectively, which may be helpful to apply this knowledge in daily work.

The paper does not address the assessment of the loudspeaker as multiple-output system namely the radiation into the 3D space. However, these important properties can be described by linear transfer functions measured between the electrical input and the sound pressure output. Using the concept of equivalent input distortion the effect of the motor and suspension distortion can easily be predicted at any point in the sound field.

Thus, the evaluation of loudspeaker performance in the 3D space and in the large signal domain is required for a comprehensive evaluation of the loudspeaker. The tools in the objective approach should be sharper and more sensitive than our human ear. The subjective approach is also required in loudspeaker design but considers influence of our auditory system. Here audibility and the impact on the perceived sound quality is investigated. Measures which consider the masking effects and other psycho-acoustical mechanisms perform a kind of data reduction of the objective information. Both objective and subjective data are required to design loudspeakers with an optimal balance between performance, size and cost.

9. REFERENCES

[1] M. Dodd, et. al., “Voice Coil Impedance as a Function of Frequency and Displacement” presented at the 117th Convention of the Audio Eng. Soc. , 2004 October 28–31 San Francisco, CA, USA.

[2] A., Chaigne, “Influence of Material and Shape on Sound Reproduction by an Electrodynamic Loudspeaker,” presented at the 118th Convention of the Audio Eng. Soc. , 2005 May 28–31, Barcelona, Spain, preprint 6420.

[3] O. Thomas, “ Analyse et modelisation de vibrations non-lineaires de milieux minces elastiques,” These of UPMC (Paris 6), (2001 October).

[4] J. Vanderkooy, “Nonlinearities in Loudspeaker Ports,” presented at the 104th Convention of the Audio Eng. Soc., 1998 May 16 – 19, Amsterdam, NL, preprint 4748.

[5] N.B. Roozen, “Reduction of Bass-Reflex Port Nonlinearities by Optimizing the Port Geometry,” presented at the 104th Convention of the Audio Eng. Soc., 1998 May 16 – 19, Amsterdam, NL, preprint 4661.

[6] L. J. Black, “A Physical Analysis of Distortion produced by the Nonlinearity of the Medium,” J. Acoust. Soc. Am. 1, 266 – 267 (1940).

[7] W. Klippel, “Nonlinear Wave Propagation in Horns and Ducts,” J. Acoust. Soc. Am. vol. 98, No. 1 , 431 – 438 (July 1995).

[8] W. Klippel, "Modeling the Nonlinearities in Horn Loudspeakers," *J. Audio Eng. Society*, vol. 44, pp. 470-480 (1996).

[9] H. J. Butterweck, “About the Doppler Effect in Acoustic Radiation from Loudspeakers,” Acustica Vol. 63, pp. 77 –79, (1987).

[10] B. Zoltogorski, “Moving Boundary Condition and Non-Linear Propagation as the Sources of Non-Linear Distortion in Loudspeaker,” presented at the 94th Convention of the Audio Eng. Soc., 1993 March 16-19, Berlin Germany, preprint 3510.

[11] D. Clark, „Precision Measurement of Loudspeaker Parameters,“ J. Audio Eng. Soc. vol. 45, pp. 129 - 140 (1997 March).

[12] W. Klippel, “Measurement of Large-Signal Parameters of Electrodynamic Transducer,” presented at the 107th Convention of the Audio Engineering Society, New York, September 24-27, 1999, preprint 5008.

[13] “Sound System Equipment. Part 5: Loudspeakers,” IEC Publication 60268-5

[14] W. Klippel, “Equivalent Input Distortion,” J. Audio Eng. Society **52**, No. 9 pp. 931-947 (2004 Sept.).

[15] R. H. Small, “Measurement of Loudspeaker Amplitude Modulation Distortion,” presented at the 114th Convention of the Audio Eng. Soc. in Amsterdam, March 22 – 25, 2003, preprint 5731.

[16] M.H. Knudsen and J.G. Jensen, “Low-Frequency Loudspeaker Models that Include Suspension Creep,” *J. Audio Eng. Soc*., vol. 41, pp. 3-18, (Jan./Feb. 1993)

[17] E. Czerwinski, et. al., "Multitone Testing of Sound System Components – Some Results and Conclusions, J. Audio Eng. Soc. vol. 49, pp. 1011 - 1048 (2001 Nov.).

[18] W. Klippel, “Assessment of Voice-Coil Peak Displacement X_{max},” J. Audio Eng. Society **51**, Heft 5, pp. 307 - 323 (2003 May).

[19] W. Klippel, "Prediction of Speaker Performance at High Amplitudes," presented at 111th Convention of the Audio Engineering Society, 2001 September 21–24, New York, NY, USA

[20] Specification of the KLIPPEL Analyzer System, Klippel GmbH, www.klippel.de, 2005.

[21] W. Klippel, „Measurement of Impulsive Distortion, Rub and Buzz and other Disturbances", preprint # 5734 presented at the 114th Convention of the Audio Engineering Society, 2003 March 22–25, Amsterdam, The Netherlands.

[22] W. Klippel, "Speaker Auralization – Subjective Evaluation of Nonlinear Distortion," presented at the 110th Convention of the Audio Engineering Society, Amsterdam, May 12-15, 2001, preprint 5310, J. Audio Eng. Society, Vol. 49, No. 6, 2001 June, P. 526.